masses between the purified peptide and the methionine sulfoxide form of CRSP-1 was 58.9 Da, we hypothesized that the C-terminal glycine is retained intact without being converted into the amide in the peptide purified in this study. To verify whether the peptide purified from peak 5 is the glycine-extended form of CRSP-1 (CRSP-1-Gly), we synthesized CRSP-1-Gly and compared the retention times of CRSP-1-Gly possessing two methionine sulfoxides with those of the purified peptide in the ion exchange and the reverse phase HPLCs. We concluded that the purified peptide was the glycine-extended form of CRSP-1, based on its retention times in the two HPLCs (data not shown).

3.2. Effects of CRSP-1-Gly on the porcine CT receptor

To compare the biological potency of synthetic CRSP-1-Gly with that of CRSP-1 on the CT receptor, we stimulated LLC-PK_1 cells as well as COS-7 cells expressing porcine CT receptor with CRSP-1-Gly or CRSP-1, and measured their cAMP production levels. As shown in Fig. 2, the dose-response curve of CRSP-1-Gly overlapped with that of CRSP-1 both in LLC-PK_1 cells and in the COS-7 cells expressing the CT receptor, indicating that CRSP-1-Gly is equipotent as CRSP-1. Although there is a possibility that CRSP-1-Gly acts on the CT receptor after conversion into CRSP-1 by alpha-amidating monooxygenase (PAM), COS-7 cells are reported to have an undetectable level of the PAM activity [24]. These data indicate that CRSP-1-Gly can directly stimulate the CT receptor even though it does not have the amide structure.

3.3. Characterization of IR-CRSP-1-Gly and IR-CRSP-1 in the porcine brain

IR-CRSP-1-Gly and IR-CRSP-1 levels in the porcine brain extracts were measured using the antiserum against CRSP-1[24–38]-NH_2 prepared in our previous study [12] and a newly prepared antiserum against CRSP-1[30–38]-Gly. Half-maximal inhibition of radioiodinated ligand binding to the antiserum against CRSP-1[30–38]-Gly was observed at 20 fmol/tube. The antisera against CRSP-1[24–38]-NH_2 and CRSP-1[30–38]-Gly have very low cross-reactivity with CRSP-1-Gly and CRSP-1, respectively (<0.1%). The acid extracts of porcine whole brain without cerebellum were separated by gel filtration HPLC, reverse phase HPLC and ion exchange HPLC, and IR-CRSP-1-Gly and IR-CRSP-1 levels in each fraction were measured using RIAs specific for CRSP-1 and CRSP-1-Gly. The retention time of IR-CRSP-1-Gly was almost identical to that of IR-CRSP-1 in the gel filtration HPLC, as molecular masses of CRSP-1-Gly (4156.9 Da) and CRSP-1 (4098.9 Da) are almost identical with each other (Fig. 3). Similarly, the retention time of IR-CRSP-1-Gly was almost identical to that of IR-CRSP-1 in the reverse phase HPLC (Fig. 4), as the conversion of the C-terminal glycine of CRSP-1-Gly into the amide did not affect their hydrophobicity in the reverse phase HPLC under the acidic

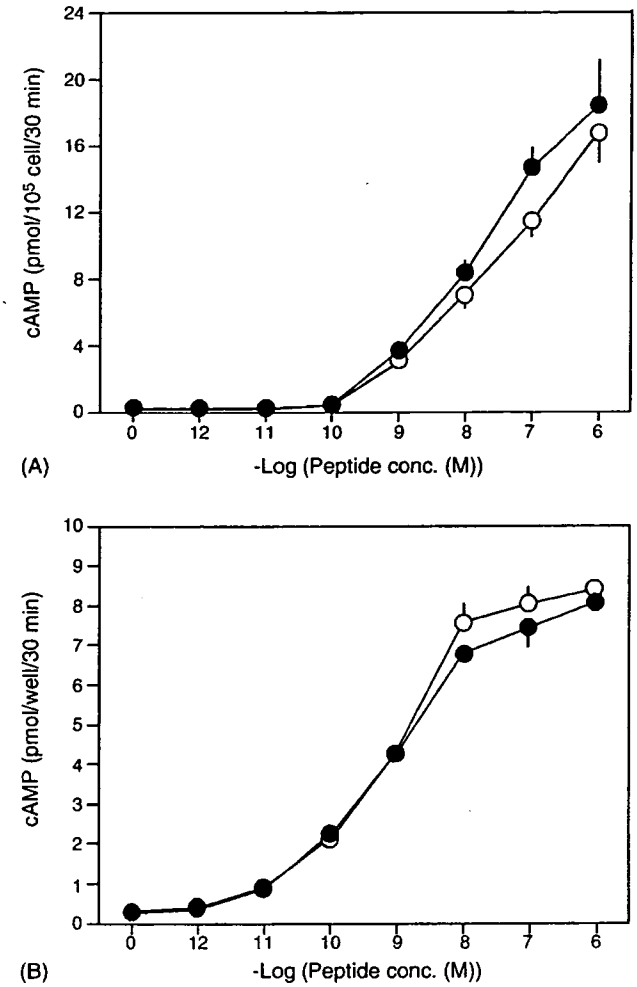

Fig. 2. Effects of CRSP-1 and CRSP-1-Gly on cAMP production in LLC-PK_1 cells (A), and COS-7 cells expressing porcine CT receptor (B). LLC-PK_1 cells as well as COS-7 cells expressing the porcine CT receptor were stimulated with the indicated concentrations of CRSP-1 (open circle) and CRSP-1-Gly (closed circle). The assay media were then succinylated, evaporated, and submitted to RIA for cAMP. Each point represents the mean ± S.E.M. of three separate determinations.

conditions. On the other hand, this C-terminal conversion increased the retention time in the CM-2SW ion exchange HPLC (Fig. 5), as the C-terminal glycine of CRSP-1-Gly carries a negative charge in the neutral pH range. The peak height of IR-CRSP-1-Gly in each HPLC was approximately 30% of that of IR-CRSP-1. This fact suggests that about one-fourth of total IR-CRSP-1 (IR-CRSP-1 plus IR-CRSP-1-Gly) is IR-CRSP-1-Gly in the porcine brain. Compared to other neuropeptides, IR-CRSP-1 and IR-CRSP-1-Gly were eluted relatively in wide ranges in each HPLC, particularly in the gel filtration HPLC and ion exchange HPLC. The wide spread elution of these immunoreactivity in the gel filtration HPLC may be due to the overload of the sample. On the other hand, the wide spread elution of the immunoreactivity in the ion exchange HPLC is probably due to the oxidation of three methionines in the sequences of CRSP-1 and CRSP-1-Gly.

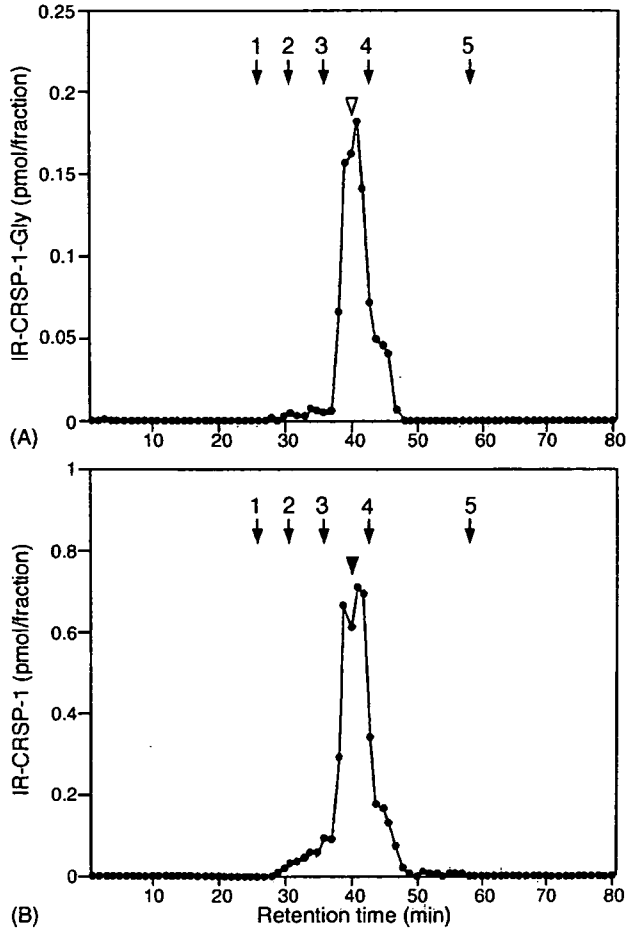

Fig. 3. Gel filtration HPLC of porcine brain extracts. The SP-III fraction of porcine brain extracts was separated by gel filtration HPLC on a TSK-gel G2000SW$_{XL}$ column (7.8 mm × 300 mm, Tosoh), eluting with 60% CH_3CN containing 0.1% TFA at a flow rate of 0.2 ml/min. Aliquots of each fraction were submitted to RIAs for CRSP-1 (A) and CRSP-1-Gly (B). Arrowheads indicate the retention times of synthetic CRSP-1-Gly (open arrowhead) and CRSP-1 (closed arrowhead). Arrows indicate the retention times of (1) BSA, (2) horse myoglobin, (3) human adrenomedullin, (4) neurotensin, and (5) acetic acid.

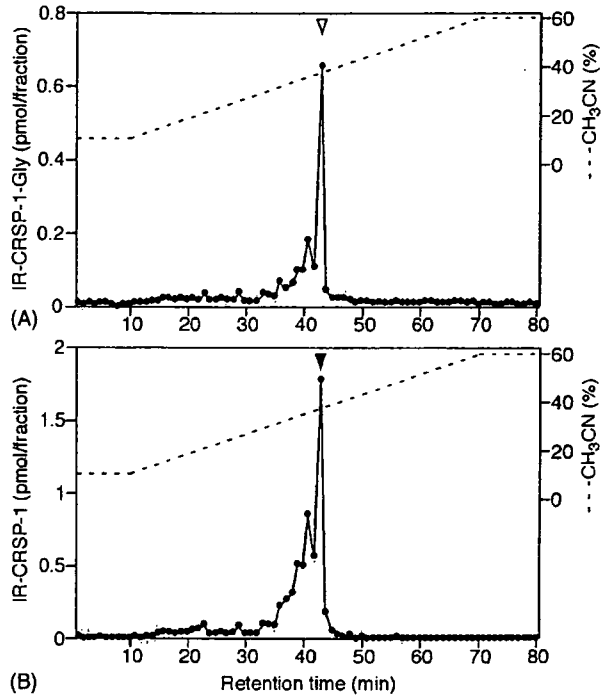

Fig. 4. Reverse phase HPLC of porcine brain extracts. Peak fractions of IR-CRSP-1 and IR-CRSP-1-Gly eluted from the gel filtration HPLC (Fig. 3) were pooled, lyophilized, and separated by reverse phase HPLC on a C_{18} column (Symmetry 300^{TM} C_{18} 5 μm, 4.6 mm × 250 mm; Waters) using a linear gradient elution of CH_3CN from 10 to 60% in 0.1% TFA at a flow rate of 1 ml/min. Aliquots of each fraction were submitted to RIAs for CRSP-1 (A) and CRSP-1-Gly (B). Arrowheads indicate the retention times of synthetic CRSP-1-Gly (open arrowhead) and CRSP-1 (closed arrowhead).

In fact, two methionines of CRSP-1 and CRSP-1-Gly were oxidized when we isolated them, indicating that at least two of three methionines are easily oxidized during the extraction and purification. We deduce that CRSP-1 and CRSP-1-Gly are not oxidized in the brain tissue, but that they are oxidized in the steps of extraction and separation.

3.4. Measurement of concentrations of IR-CRSP-1-Gly, IR-CRSP-1, IR-CRSP-2 and IR-CRSP-3 in porcine tissues

We next evaluated the tissue levels of IR-CRSP-1-Gly and IR-CRSP-1, using the antisera specific for each peptide. In addition, we prepared antisera against CRSP-2[29–37]-NH_2 and CRSP-3[29–37]-NH_2 to measure the tissue concentrations of CRSP-2 and CRSP-3. Half-maximal inhibition of radioiodinated ligand binding to antisera against CRSP-2[29–37]-NH_2 or CRSP-3[29–37]-NH_2 was observed at 20 fmol/tube or 50 fmol/tube, respectively, and their N-terminal extensions, i.e. CRSP-2 and CRSP-3, did not alter sensitivity of each RIA. The antisera against CRSP-1[24–38]-NH_2, CRSP-1[30–38]-Gly, CRSP-2[29–37]-NH_2 and CRSP-3[29–37]-NH_2 have very low cross-reactivity with all these antigens (<0.1%) except for each antigen used for the immunization. Using these antisera, we measured the tissue concentrations of IR-CRSP-1-Gly, IR-CRSP-1, IR-CRSP-2 and IR-CRSP-3, and calculated the ratio in the tissue concentration of IR-CRSP-1-Gly to total IR-CRSP-1 (Table 1). More than 0.2 pmol/g wet tissue of IR-CRSP-1-Gly was detected in all tissues except for the cerebellum. More than 1 pmol/g wet tissue of IR-CRSP-1-Gly was detected in the midbrain, hypothalamus, anterior and posterior lobes of pituitary and thyroid gland, where a relatively high concentration of CRSP-1 was observed (>6 pmol/g wet tissue). The highest concentration of IR-CRSP-1-Gly was detected in the posterior lobe of pituitary (5.39 ± 0.57 pmol/g wet tissue). The ratio of IR-CRSP-1-Gly to the total IR-CRSP-1 varies from 0.02 to 0.35, and the highest ratio (0.35) was observed in the hippocampus and olfactory bulb.

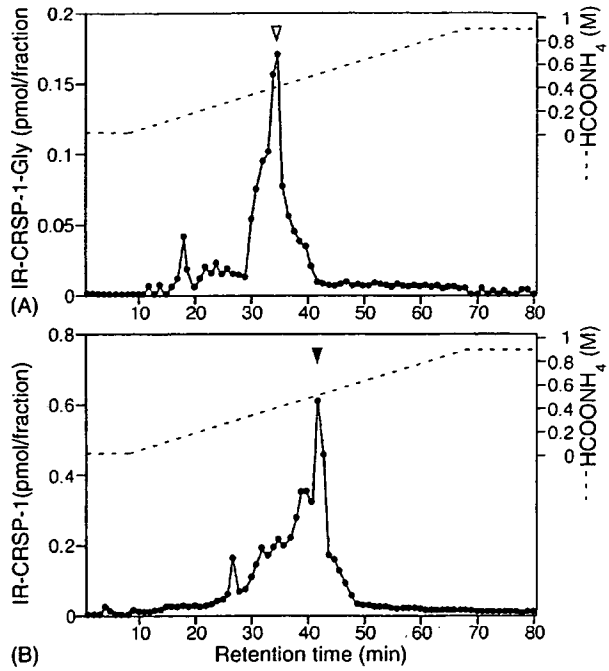

Fig. 5. Cation exchange HPLC of porcine brain extracts. Peak fractions of CRSP-1 and CRSP-1-Gly eluted from the gel filtration HPLC (Fig. 3) were pooled, lyophilized, and separated by CM ion exchange HPLC (TSK-gel CM-2SW, 7.8 mm × 300 mm; Tosoh) eluting with a linear gradient elution of $HCOONH_4$ (pH 6.5) from 9 mM to 0.9 M containing 10% CH_3CN at a flow rate of 2 ml/min. Aliquots of each fraction were lyophilized and submitted to RIAs for CRSP-1 (A) and CRSP-1-Gly (B). Arrowheads indicate the retention times of synthetic CRSP-1-Gly (open arrowhead) and CRSP-1 (closed arrowhead).

On the other hand, more than 1 pmol/g wet tissue of IR-CRSP-2 was observed in the midbrain, hypothalamus, anterior and posterior lobes of pituitary and thyroid gland, and the tissue concentrations of IR-CRSP-2 were comparable to those of IR-CRSP-1-Gly. However, significant levels of IR-CRSP-3 were observed only in the anterior and posterior lobes of pituitary and hypothalamus, and those in the other brain regions were less than the limit of quantitative measurement.

4. Discussion

Many biologically active peptides possess the C-terminal amide structure, and in most of the amidated peptides, such as oxytocin [7], gastrin [17], thyrotropin releasing hormone [19] and CT [22], the C-terminal amide structure is shown to be essential for eliciting their full biological activity. These facts imply that the strong interaction exists between the C-terminal amide structure of these peptides and the ligand binding site of their receptors. As shown in Fig. 2, however, we demonstrated that the glycine-extended form of CRSP-1 is as potent as CRSP-1 on both the endogenously expressed and recombinantly expressed CT receptors. This result indicates that no interaction exists between the C-terminal end of CRSP-1 and the ligand binding site of the CT receptor. We have already shown that the precursors of bovine and canine CRSP-1s do not have a donor glycine for the amidation, but synthetic bovine and canine CRSP-1s lacking the C-terminal amide can stimulate the CT receptor at a potency comparable to that of amidated porcine CRSP-1 [11]. In the limited cases of the amidated peptides, such as vasointestinal polypeptide [6,8], PHI [5] and secretin [18] of the same peptide family, the C-terminal amide structure is not essential for eliciting their activity. CRSP-1 is considered to belong to this exceptional case, and is the first exception in the CGRP family, as the C-terminal amidation is essential for eliciting its activity in the other members of the CGRP family [4,14,22,23].

Relatively high concentrations of IR-CRSP-1-Gly were detected in the tissues and brain regions, such as the midbrain, hypothalamus, anterior and posterior lobes of pituitary and thyroid gland (>1 pmol/g wet tissue), where high concentrations of IR-CRSP-1 (>6 pmol/g wet tissue) were also observed (Table 1). Based on these results, the relative ratio in the tissue concentration of IR-CRSP-1-Gly to total IR-CRSP-1 was calculated to be 0.02–0.35 in each region and tissue. The ratio of IR-CRSP-1-Gly to total IR-CRSP-1 was the lowest in the posterior lobe of pituitary and thyroid gland, which contained the highest levels of IR-CRSP-1 (>60 pmol/g wet weight). In contrast, all brain regions and the anterior lobe of pituitary contain IR-CRSP-1-Gly at higher

Table 1
Concentrations (pmol/g wet weight) of IR-CRSP-1-Gly, IR-CRSP-1, IR-CRSP-2 and IR-CRSP-3 in porcine tissues, and ratio of IR-CRSP-1-Gly to total IR-CRSP-1

Tissue	CRSP-1-Gly	CRSP-1	CRSP-2	CRSP-3	CRSP-1-Gly/total CRSP-1
Cerebral cortex	<0.2	0.33 ± 0.01	0.27 ± 0.04	<0.2	ND
Cerebellum	0.21 ± 0.05	<0.2	0.46 ± 0.23	<0.2	ND
Midbrain	1.40 ± 0.04	7.53 ± 0.72	1.02 ± 0.20	<0.2	0.16
Hippocampus	0.51 ± 0.04	0.97 ± 0.04	0.38 ± 0.11	<0.2	0.35
Caudate nucleus	0.49 ± 0.04	1.31 ± 1.67	0.69 ± 0.19	<0.2	0.27
Thalamus	0.70 ± 0.4	3.67 ± 0.11	0.71 ± 0.20	<0.2	0.16
Hypothalamus	1.44 ± 0.07	6.57 ± 1.21	1.25 ± 0.23	0.20 ± 0.04	0.18
Pons/medulla oblongata	0.53 ± 0.01	1.86 ± 0.20	0.42 ± 0.10	<0.2	0.22
Olfactory bulb	0.24 ± 0.04	0.45 ± 0.06	0.45 ± 0.14	<0.2	0.35
Pituitary, anterior	2.50 ± 0.11	11.56 ± 1.44	1.29 ± 0.34	0.67 ± 0.08	0.18
Pituitary, posterior	5.39 ± 0.57	109.88 ± 25.99	4.56 ± 0.45	2.85 ± 0.52	0.05
Thyroid gland	1.33 ± 0.37	66.78 ± 26.19	1.46 ± 0.75	<0.2	0.02

Each value represents mean ± S.E.M. ($n = 3$). ND, not determined.

ratios of 0.16–0.35. Consistent with these ratios, the peak height of IR-CRSP-1-Gly observed in each HPLC of the characterization (Figs. 3–5) was approximately 30% that of IR-CRSP-1, indicating that CRSP-1-Gly is present as one of the major endogenous forms and can act on the cells expressing CT receptor. In the hypothalamus, pituitary and thyroid gland, PAM is known to be abundantly expressed [1,2,16,20,21]. On the other hand, the conversion rate of Tyr-Gly-Gly into Tyr-Gly-amide by PAM was reported to be much lower than that of Tyr-X-Gly into Tyr-X-amide (X = aromatic or aliphatic residue) [3]. To elucidate the differences in the ratio of CRSP-1 to CRSP-1-Gly in each tissue and brain region, it is essential to identify CRSP-1-expressing cells and to compare them with the PAM-expressing cells in the brain, pituitary and thyroid gland, in addition to the kinetic analysis for PAM in the conversion of CRSP-1-Gly into CRSP-1.

In the Northern blot analysis of CRSP-2 and CRSP-3, the band intensities of CRSP-2 and CRSP-3 mRNAs in each brain region were comparable to and about one-fifth that of CRSP-1, respectively (unpublished observation). We expected that the tissue concentration of IR-CRSP-2 and IR-CRSP-3 in the brain and thyroid gland was comparable to and about 20% that of IR-CRSP-1, respectively. However, the tissue concentrations of IR-CRSP-2 and IR-CRSP-3 in the brain, pituitary and thyroid gland are far lower than those estimated from Northern blot analysis data (Table 1). As the precursors of CRSP-2 and CRSP-3 do not possess a typical prohormone convertase cleavage site on the N-terminal side of each peptide, we surmised that the majority of IR-CRSP-2 and IR-CRSP-3 was present as their precursor forms in the cells and tissues. Therefore, tissue concentrations of IR-CRSP-2 and IR-CRSP-3 could be underestimated, because the extraction efficiency of the precursors is generally lower than those of the processed peptides.

In the present study, we isolated a new biologically active peptide from porcine brain extracts by monitoring the cAMP production in LLC-PK_1 cells, and this peptide was verified to be a glycine-extended form of CRSP-1 by the following structural analyses. Interestingly, CRSP1-Gly is equipotent as CRSP-1 and is present in all the examined tissues and brain regions along with CRSP-1 at a relatively high ratio. These facts raise the possibility that CRSP-1-Gly is not as an intermediate but an endogenous hormone and neuropeptide stimulating the CT receptor. To address this issue, more elaborate biochemical characterization, immunohistochemical and physiological analyses of CRSP-1-Gly are required to identify its physiological significance by contrasting with those of CRSP-1.

Acknowledgements

This work was supported in part by research grants from the Ministry of Education, Culture, Sports, Science and Technology (Special Coordination Funds for the Promotion of Science and Technology), from the Ministry of Health, Labor and Welfare (Cardiovascular Diseases), from the Pharmaceuticals and Medical Devices Agency (Medical Frontier Project) of Japan, and from the Protein Research Foundation (Kaneko-Narita Research Grant). The authors are grateful to Ms. A. Okabe, Y. Takada and S. Fujiwara of this institute for their technical assistance.

References

[1] Braas KM, Harakall SA, Ouafik L, Eipper BA, May V. Expression of peptidylglycine alpha-amidating monooxygenase: an in situ hybridization and immunocytochemical study. Endocrinology 1992;130:2778–88.
[2] Braas KM, Stoffers DA, Eipper BA, May V. Tissue specific expression of rat peptidylglycine alpha-amidating monooxygenase activity and mRNA. Mol Endocrinol 1989;3:1387–98.
[3] Bradbury AF, Smyth DG. Substrate specificity of an amidating enzyme in porcine pituitary. Biochem Biophys Res Commun 1983;112:372–7.
[4] Carpenter KA, Schmidt R, von Mentzer B, Haglund U, Roberts E, Walpole C. Turn structures in CGRP C-terminal analogues promote stable arrangements of key residue side chains. Biochemistry 2001;40:17–25.
[5] Cauvin A, Vandermeers-Piret MC, Vandermeers A, Coussaert E, de Neef P, Robberecht P, et al. Rat PHI, PHI-GLY and PHV (1–42) stimulate adenylate cyclase in six rat tissue and cell membranes. Peptides 1990;11:1009–14.
[6] Fahrenkrug J, Ottesen B, Palle C. Non-amidated forms of VIP (glycine-extended VIP and VIP-free acid) have full bioactivity on smooth muscle. Regul Pept 1989;26:235–9.
[7] Ferrier BM, du Vigneaud V. 9-Deamidooxytocin, an analog of the hormone containing a glycine residue in place of the glycinamide residue. J Med Chem 1966;9:55–7.
[8] Gafvelin G, Andersson M, Dimaline R, Jornvall H, Mutt V. Isolation and characterization of a variant form of vasoactive intestinal polypeptide. Peptides 1988;9:469–74.
[9] Hull RN, Cherry WR, Weaver GW. The origin and characteristics of a pig kidney cell strain, LLC-PK. In Vitro 1976;12:670–7.
[10] Katafuchi T, Hamano K, Kikumoto K, Minamino N. Identification of second and third calcitonin receptor-stimulating peptide in porcine brain. Biochem Biophys Res Commun 2003;308:445–51.
[11] Katafuchi T, Hamano K, Minamino N. Identifcation, structural determination, and biological activity of bovine and canine calcitonin receptor-stimulating peptides. Biochem Biophys Res Commun 2004;313:74–9.
[12] Katafuchi T, Kikumoto K, Hamano K, Kangawa K, Matsuo H, Minamino N. Calcitonin receptor-stimulating peptide, a new member of the calcitonin gene-related peptide family. Its isolation from porcine brain, structure, tissue distribution, and biological activity. J Biol Chem 2003;278:12046–54.
[13] Kikumoto K, Katafuchi T, Minamino N. Specificity of porcine calcitonin receptor and calcitonin receptor-like receptor in the presence of receptor-activity-modifying proteins. Hypertens Res 2003;26:S15–23.
[14] Kitamura K, Kato J, Kawamoto M, Tanaka M, Chino N, Kangawa K, et al. The intermediate form of glycine-extended adrenomedullin is the major circulating molecular form in human plasma. Biochem Biophys Res Commun 1998;244:551–5.
[15] Lin HY, Harris TL, Flannery MS, Aruffo A, Kaji EH, Gorn A, et al. Expression cloning of an adenylate cyclase-coupled calcitonin receptor. Science 1991;254:1022–4.
[16] May V, Ouafik L, Eipper BA, Braas KM. Immunocytochemical and in situ hybridization studies of peptidylglycine alpha-amidating monooxygenase in pituitary gland. Endocrinology 1990;127:358–64.

[17] McGuigan JE, Thomas HF. Physiological and immunological studies with desamidogastrin. Gastroenterology 1972;62:553–8.
[18] Olson H, Lind P, Pohl G, Henrichson C, Mutt V, Jornvall H, et al. Production of a biologically active variant form of recombinant human secretin. Peptides 1988;9:301–7.
[19] Pekary AE, Stephens R, Simard M, Pang XP, Smith V, DiStefano Jr J, et al. Release of thyrotropin and prolactin by a thyrotropin-releasing hormone (TRH) precursor, TRH-Gly: conversion to TRH is sufficient for in vivo effects. Neuroendocrinology 1990;52:618–25.
[20] Prigge ST, Kolhekar AS, Eipper BA, Mains RE, Amzel LM. Amidation of bioactive peptides: the structure of peptidylglycine alpha-hydroxylating monooxygenase. Science 1997;278:1300–5.
[21] Prigge ST, Mains RE, Eipper BA, Amzel LM. New insights into copper monooxygenases and peptide amidation: structure, mechanism and function. Cell Mol Life Sci 2000;57:1236–59.
[22] Rittel W, Maier R, Brugger M, Kamber B, Riniker B, Sieber P. Structure-activity relationship of human calcitonin. III. Biological activity of synthetic analogues with shortened or terminally modified peptide chains. Experientia 1976;32:246–8.
[23] Roberts AN, Leighton B, Todd JA, Cockburn D, Schofield PN, Sutton R. et al. Molecular and functional characterization of amylin, a peptide associated with type 2 diabetes mellitus. Proc Natl Acad Sci USA 1989;86:9662–6.
[24] Tateishi K, Arakawa F, Misumi Y, Treston AM, Vos M, Matsuoka Y. Isolation and functional expression of human pancreatic peptidylglycine alpha-amidating monooxygenase. Biochem Biophys Res Commun 1994;205:282–90.

Fusogenic Liposome can be Used as an Effective Vaccine Carrier for Peptide Vaccination to Induce Cytotoxic T Lymphocyte (CTL) Response

Toshiki SUGITA,[a,e] Tomoaki YOSHIKAWA,[a,e] Jian-Qing GAO,[a] Mariko SHIMOKAWA,[e] Atushi ODA,[a,e] Takako NIWA,[a,e] Mitsuru AKASHI,[b,e] Yasuo TSUTSUMI,[c,e] Tadanori MAYUMI,[d] and Shinsaku NAKAGAWA*[,a,e]

[a] *Department of Biopharmaceutics, Graduate School of Pharmaceutical Sciences, Osaka University; 1–6 Yamadaoka, Suita, Osaka 565–0871, Japan:* [b] *Department of Molecular Chemistry, Graduate School of Engineering, Osaka University; 2–1 Yamadaoka, Suita, Osaka 565–0871, Japan:* [c] *National Institute of Health Science, Osaka Branch Fundamental Research Laboratories for Development of Medicine; 1–1–43 Hoenzaka, Chuo-ku, Osaka 540–0006, Japan:* [d] *Department of Cell Therapeutics, Graduate School of Pharmaceutical Sciences, Kobe-Gakuin University; 518 Arise, Igawadani, Nishi-ku, Kobe 651–2180, Japan: and* [e] *CREST (Core Research for Evolutional Science and Technology) of Japan Science and Technology Corporation; Tokyo, 102–8666, Japan.*

Received August 18, 2004; accepted October 18, 2004; published online October 20, 2004

We reported previously that fusogenic liposome (FL) introduced antigen protein encapsulated in the liposome directly into the cytoplasm of the antigen presenting cells, and that it induced immune responses. In the present study, we encapsulated TAX38-46, an HTLV-I derived protein and an antigen peptide model, into FL. The ability to induce effective cytotoxic T lymphocytes (CTL) responses in immunized mice was evaluated. Results showed FL could induce CTL response effectively and suggested that FL is a potential peptide vaccine carrier.

Key words fusogenic liposome; cytotoxic T lymphocyte (CTL); peptide vaccine

Induction of cytotoxic T lymphocytes (CTL) that kill tumor cells is a critical role of immunotherapeutic agents for cancer. Most cancer vaccine strategies have focused on induction of CTL and various approaches, including DNA, virus vector or peptide vaccine, have been tested.[1)] In general, the advantages of a peptide vaccine are the induction of CTL by the epitope and the safety, stability and simplicity of peptide production. However, peptides by themselves are rather weak immunogens. Peptides usually require the addition of an adjuvant for inducing immunogenicity, and recently, incomplete Freund's adjuvant (IFA) has been widely used as a vaccine adjuvant in clinical research.[2)] However, IFA is only useful for inducing humoral immunity and thus it does not induce effective cell-mediated immune responses. In contrast, complete Freund's adjuvant (CFA) is used for CTL induction, although it cannot be applied clinically due to serious side effects, such as inflammation.[3)]

To induce cell-mediated immune responses, a peptide must be delivered through the cytoplasm to the MHC class I processing pathway. However, peptides are unable to pass through the cytoplasm alone.[4)] Therefore, we hypothesized that a vaccine carrier is required, which can deliver antigens into the cytoplasm and which exhibits adjuvant activity. We reported previously that fusogenic liposome (FL) introduces antigen protein encapsulated in the liposome directly into the cytoplasm, and that it can induce effective immune responses.[5—7)] FL is a fusion liposome in which proliferating ability is inactivated, but which retains its cell membrane fusing ability. Therefore, FL can deliver encapsulated molecules into cells. Furthermore, FL possesses immune stimulating activity.[5)] In this context, we considered FL as an ideal peptide vaccine carrier.

In the present study, we chose the TAX protein epitope (TAX 38-46; H-2D^{k-} restricted epitope in TAX, amino acid residues 38-46, sequence ARLHRHALL.[10)]), which is an immunodominant target antigen derived from the human T-cell leukemia virus type 1 (HTLV-I), as a model peptide. HTLV-I, a retro virus, is known to cause Adult T-cell leukemia (ATL).[8)] ATL is characterized by poor prognosis after chemotherapy and no effective therapy exists. Immunotherapy, which can induce strong anti HTLV-I CTL, has been proposed as an optimal approach to ATL treatment.[9)] However, an effective immunotherapeutic approach has not been developed to date.

MATERIALS AND METHODS

Cells and Animals L929 cells were cultured with RPMI-1640 containing with 10% fetal calf serum (FCS). Female C3H mice were purchased from Nippon SLC (Kyoto, Japan) and used at 6 weeks-old stage.

Fusogenic Liposome Encapsulated TAX 38-46 TAX 38-46 and FITC conjugated TAX 38-46 were purchased from SIGMA (Japan). FL was prepared as described previously.[5—7)] Briefly, lipid mixture (L-α-dimyristoyl phosphatidic acid/phosphatidylcholine/cholesterol in molar ratio of 1 : 4 : 5) was hydrated with phosphate buffered saline (PBS) or PBS containing TAX 38-46 or FITC conjugated TAX 38-46. Peptides containing liposome was prepared from these hydrated mixture by using a hand-held extruder with two layers of cellulose acetate membranes (pore size, 800 nm in diameter) (ADVANTEC, Osaka, Japan), and washed with PBS by centrifugation (20000 rpm, 40 min, 4 °C) in order to remove free peptides. These liposomes were mixed with UV-inactivated Sendai virus and incubated at 37 °C for 2 h with shaking. FL was purified by sucrose gradient centrifugation (24000 rpm, 2 h, 4 °C). The diameter of FL was detected by using ZETASIZER 3000HS (Malvern, U.K.). The concentration of peptide in FL was determined by measuring the fluorescence intensity of FITC.

^{51}Cr Release Assay For the CTL assay, TAX38-46 (50 μg), empty FL, TAX38-46 emulsified with CFA (contains 50 μg

* To whom correspondence should be addressed. e-mail: nakagawa@phs.osaka-u.ac.jp

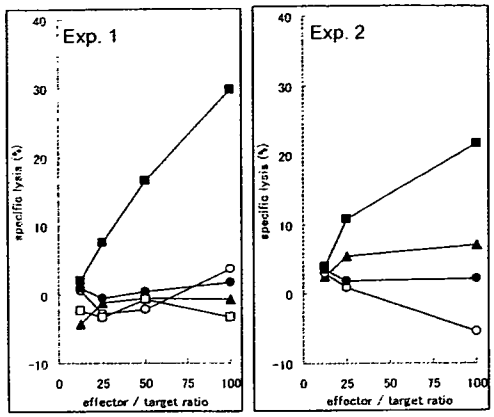

Fig. 1. TAX Peptide Encapsulated in FL Induced TAX Specific CTL

Nine days after the final immunization, mononuclear cells from the spleen of mice immunized with PBS (closed circle), TAX 38-46 alone (open circle), empty FL (open square), TAX 38-46 emulsified with CFA (closed triangle), or TAX 38-46 encapsulated in FL (closed square) were isolated and restimulated with MMC-treated TAX38-46 pulsed L929 for 5 d to enhance the frequency of antigen specific CTLs. CTL activity against TAX38-46 pulsed L929 (positive targets) or L929 (negative targets) was measured by ^{51}Cr release assay. Results were expressed as a percentage of specific lysis. Percentage of specific lysis=(percentage of positive target lysis)−(percentage of negative target lysis).

TAX38-46), or TAX38-46 encapsulated in FL (contains 30 μg TAX38-46) diluted to in total were injected into back of C3H mice (i.d.), respectively. Mice were immunized once a week for three weeks, and the spleen was harvested 9 d after the last immunization. Splenocytes were mixed with mitomycin C (MMC) treated TAX38-46 pulsed L929 for 5 d, and CTL assay was determined as follows. L929 cells (5×10^6) were pulsed with TAX 38-46 (positive targets) for 1 h at 37 °C or not (negative targets), and labeled with 200 μCi of ^{51}Cr for 2 h at 37 °C. Splenocytes were incubated with target cells (positive or negative targets) for 2 h at 37 °C. CTL activity was determined by measuring ^{51}Cr levels in the supernatants using a gamma counter. The specific lysis was determined as follows: percentage of specific lysis= (percentage of positive target lysis)−(percentage of negative target lysis).

RESULTS AND DISCUSSION

We prepared the FL encapusulating TAX 38-46. The diameter of FL was 880.1±9.5 nm. We calculated the concentrarion of peptide in FL using FITC conjugated TAX38-46. One milliliter of FL suspension at OD_{540} of 1.0 contained 29.8 μg of TAX 38-46. FL encapsulating TAX 38-46 was immunized with 100 μl at OD_{540} of 10.0.

Figure 1 demonstrates that the induction of TAX-specific CTL occurred only in response to TAX38-46-FL. CTL induction could not be detected in the TAX38-46-CFA administered group, in the TAX38-46 group, or in the empty FL group. Likewise, there was no CTL response in the group immunized with the mixture of TAX 38-46 and empty FL (data not shown). Previous reports have demonstrated that FL can deliver peptide directly into cytoplasm and that it possesses immune stimulating ability.

In a future study, we will investigate the control of peptide distribution in the cytoplasm and attempt to induce a stronger CTL response. Peptides that target the endoplasmic reticulum (ER) are able to induce stronger CTL responses because MHC class I molecules are expressed on the ER membrane.[11—13] However, because FL cannot control peptide distribution in the cytoplasm, we were unable to target the ER specifically. Therefore, the use of both FL and ER targeting sequences will more effectively induce CTL.

Acknowledgements We are grateful to Mr. M. Mori and Mr. K. Sakaguchi at NOF Corporation for supplying us with lipid mixture. This work was supported in part by "Creation of bio-devices and bio-systems with chemical and biological molecules for medical use", CREST, JST.

REFERENCES

1) Berzofsky J. A., Terabe M., Oh S., Belyakov I. M., Ahlers J. D., Janik J. E., Morris J. C., *J Clin. Invest.*, **113**, 1515—1525 (2004).
2) Romero P., Cerottini J. C., Speiser D. E., *Cancer Immunol. Immunother.*, **53**, 249—255A (2004).
3) Claassen E., de Leeuw W., de Greeve P., Hendriksen C., Boersma W., *Res. Immunol.*, **143**, 478—483 (1992)
4) Harding C. V., *Curr. Opin. Immunol.*, **3**, 3—9 (1991).
5) Hayashi A., Nakanishi T., Kunisawa J., Kondoh M., Imazu S., Tsutsumi Y., Tanaka K., Fujiwara H., Hamaoka T., Mayumi T., *Biochem. Biophys. Res. Commun.*, **261**, 824—828 (1999).
6) Nakanishi T., Hayashi A., Kunisawa J., Tsutsumi Y., Tanaka Y., Yashiro-Ohtani Y., Nakanishi M., Fujiwara H., Hamaoka T., Mayumi T., *Eur. J. Immunol.*, **30**, 1740—1747 (2000).
7) Kunisawa J., Nakanishi T., Takahashi I., Okudaira A., Tsutsumi Y., Katayama K., Nakagawa S., Kiyono H., Mayumi T., *J. Immunol.*, **167**, 1406—1412 (2001).
8) Matsuoka M., *Oncogene*, **22**, 5131—5140 (2003).
9) Hanon E., Hall S., Taylor G. P., Saito M., Davis R., Tanaka Y., Usuku K., Osamu M., Weber J. N., Bangham C. R., *Blood*, **95**, 1386—1392 (2000).
10) Lomas M., Hanon E., Tanaka Y., Bangham C. R., Gould K. G., *J. Gen. Virol.*, **83**, 641—650 (2002).
11) Minev B. R., Chavez F. L., Dudouet B. M., Mitchell M. S., *Eur. J. Immunol.*, **30**, 2115—2124 (2000).
12) Moroi Y., Mayhew M., Trcka J., Hoe M. H., Takechi Y., Hartl F. U., Rothman J. E., Houghton A. N., *Proc. Natl. Acad. Sci. U.S.A.*, **97**, 3485—3490 (2000).
13) MacAry P. M., Javid B., Floto R. A., Smith K. G., Oehlmann W., Singh M., Lehner P. J., *Immunity*, **20**, 95—106 (2004).

ARTICLE IN PRESS

Available online at www.sciencedirect.com

SCIENCE DIRECT®

ELSEVIER

Biochemical and Biophysical Research Communications 328 (2005) 1043–1050

BBRC

www.elsevier.com/locate/ybbrc

A single intratumoral injection of a fiber-mutant adenoviral vector encoding interleukin 12 induces remarkable anti-tumor and anti-metastatic activity in mice with Meth-A fibrosarcoma☆

Jian-Qing Gao[a,b], Toshiki Sugita[a], Naoko Kanagawa[a], Keisuke Iida[a], Yusuke Eto[a], Yoshiaki Motomura[a], Hiroyuki Mizuguchi[c], Yasuo Tsutsumi[c], Takao Hayakawa[d], Tadanori Mayumi[e], Shinsaku Nakagawa[a,*]

[a] *Department of Biopharmaceutics, Graduate School of Pharmaceutical Sciences, Osaka University, 1-6 Yamadaoka, Suita, Osaka 565-0871, Japan*
[b] *Department of Pharmaceutics, College of Pharmaceutical Sciences, Zhejiang University, 353 Yan-an Road, Hangzhou, Zhejiang 310031, PR China*
[c] *National Institute of Health Sciences, Osaka Branch Fundamental Research Laboratories for Development of Medicine, 1-1-43 Hoenzaka, Chuo-ku, Osaka 540-0006, Japan*
[d] *National Institute of Health Sciences, 1-18-1 Kamiyoga, Setagaya-ku, Tokyo 158-8501, Japan*
[e] *Department of Cell Therapeutics, Graduate School of Pharmaceutical Sciences, Kobe-gakuin University, 518 Arise, Igawadani, Nishiku, Kobe 651-2180, Japan*

Received 12 January 2005

Abstract

Cytokine-encoding viral vectors are considered to be promising in cancer gene immunotherapy. Interleukin 12 (IL-12) has been used widely for anti-tumor treatment, but the administration route and tumor characteristics strongly influence therapeutic efficiency. Meth-A fibrosarcoma has been demonstrated to be insensitive to IL-12 treatment via systemic administration. In the present study, we developed an IL-12-encoding fiber-mutant adenoviral vector (AdRGD-IL-12) that showed enhanced gene transfection efficiency in Meth-A tumor cells, and the production of IL-12 p70 in the culture supernatant from transfected cells was confirmed by ELISA. In therapeutic experiments, a single low-dose (2×10^7 plaque-forming units) intratumoral injection of AdRGD-IL-12 elicited pronounced anti-tumor activity and notably prolonged the survival of Meth-A fibrosarcoma-bearing mice. Immunohistochemical staining revealed that the IL-12 vector induced the accumulation of T cells in tumor tissue. Furthermore, intratumoral administration of the vector induced an anti-metastasis effect as well as long-term specific immunity against syngeneic tumor challenge.

Keywords: Interleukin 12; Meth-A fibrosarcoma; Recombinant adenoviral vector; Anti-tumor; Anti-metastasis; Intratumoral administration; IL-12 insensitive

The immunostimulating cytokine interleukin 12 (IL-12), a heterodimeric protein composed of two disulfide-linked subunits, is secreted by dendritic cells as well as macrophages and is a key mediator of immunity [1,2]. A variety of studies have focused on the use of IL-12 in cancer therapy and, in these experiments, IL-12 has exhibited potent anti-tumor activity in a number of tumor models [3–5]. IL-12 acts on T and natural killer (NK) cells by enhancing the generation and activity of cytotoxic T lymphocytes and inducing the proliferation and production of cytokines, especially interferon-γ

☆ *Abbreviations:* Ad vector, adenoviral vector; AdRGD, RGD fiber-mutant Ad vector; FBS, fetal bovine serum; IL-12, interleukin 12; MOI, multiplicity of infection; PBS, phosphate-buffered saline; PFU, plaque-forming units; $TCID_{50}$, tissue culture infectious $dose_{50}$.

* Corresponding author. Fax: +81 6 6879 8179.
E-mail address: nakagawa@phs.osaka-u.ac.jp (S. Nakagawa).

0006-291X/$ - see front matter © 2005 Elsevier Inc. All rights reserved.
doi:10.1016/j.bbrc.2005.01.061

[6]. In addition, IL-12 inhibits tumor angiogenesis mainly through IFN-γ-dependent production of the chemokine interferon-inducible protein-10 (IP-10) [7].

Several mechanisms of the anti-tumor activity of IL-12 have been identified, and each contributes differently to the overall therapeutic outcome in a given tumor model [8–10]. Further, some tumor models, such as Meth-A and MCH-1A1 cells, are resistant to treatment with systemically administered IL-12 [11,12]. For example, intraperitoneal administration of murine recombinant IL-12 failed to inhibit the growth of Meth-A fibrosarcoma, even at a dosage of 500 ng daily for 3 days [11]. Compared with so-called IL-12-sensitive tumor cells such as OV-HM ovarian carcinoma and CSA1M fibrosarcoma, which both exhibited notable tumor regression after IL-12-stimulated T-cell infiltration into tumor tissues, Meth-A and MCH-1-A1 tumors lacked similar accumulation of immune cells [12]. Furthermore, otherwise exciting tumor regression results from preclinical studies were moderated by the severe adverse effects that occurred after systemic administration of IL-12 in murine models [13]. The clinical development of IL-12 as a single recombinant protein for systemic therapy has been tempered by pronounced toxicity and disappointing anti-tumor effects [14].

Intratumoral administration of IL-12 may offer several potential advantages over systemic dosing, such as delivery of the gene directly to the tissue of interest and avoidance of the drawbacks of systemic delivery, including the induction of toxicity, acute allergic reactions, and other adverse effects due to the encoded gene [15]. The results of one clinical trial suggest that intratumoral injection of $\leqslant 3 \times 10^{12}$ viral particles of an IL-12-encoding adenoviral vector in patients with advanced gastrointestinal malignancies is feasible and well tolerated [16].

In the present study, we constructed a recombinant adenovirus (Ad) vector that encoded IL-12 (AdRGD-IL-12); the gene transfection efficiency of AdRGD-IL-12 was higher than that of a conventional Ad vector. We also investigated the feasibility of using a single intratumoral injection of AdRGD-IL-12 to provide effective cancer treatment for primary and metastatic Meth-A fibrosarcoma. Furthermore, immunostaining was used to measure the postinjection infiltration of immune cells into tumor tissue.

Materials and methods

Cell lines and animals. Meth-A fibrosarcoma cells (BALB/c origin) were kindly provided by Dr. Hiromi Fujiwara (School of Medicine, Osaka University, Osaka, Japan) and were maintained by intraperitoneal passage in syngeneic BALB/c mice. Human embryonic kidney (HEK) 293 cells were cultured in DMEM supplemented with 10% FBS. BALB/c female mice were obtained from SLC (Hamamatsu, Japan) and used at 6–8 weeks of age. All of the experimental procedures were performed in accordance with the Osaka University guidelines for the welfare of animals in studies of experimental neoplasia.

Vector construction. The replication-deficient AdRGD vector was based on the adenovirus serotype 5 backbone with deletions of E1/E3 region. The RGD sequence for αv-integrin targeting was inserted into the HI loop of the fiber knob by using a two-step method, as previously described [17]. AdRGD-Luc, which is identical to the AdRGD-IL-12 vectors but with the substitution of the luciferase gene expression cassette for the cytokine, was used as negative control vector in the present study. The replication-deficient AdRGD-IL-12, which carries the murine IL-12 gene derived from mIL-12 BIA/pBluescript II KS(−) [18] (kindly provided by Prof. Hiroshi Yamamoto, Graduate School of Pharmaceutical Sciences, Osaka University, Suita, Japan), was constructed by an improved in vitro ligation method using pAdHM15-RGD [19,20]. The expression cassette, which was designed to be transcribed in order from the IL-12 p35 cDNA through the internal ribosome entry site sequence to the IL-12 p40 cDNA under the control of the cytomegalovirus promoter, was inserted into the E1-deletion region of the E1/E3-deleted Ad vector (Fig. 1). All vectors were propagated in HEK293 cells, purified by two rounds of CsCl gradient centrifugation, dialyzed with phosphate-buffered saline (PBS) containing 10% glycerol, and stored at −80 °C. The number of viral particles in vector stock was determined spectrophotometrically by the method of Maizel et al. [21]. Titers (tissue culture infectious $dose_{50}$; $TCID_{50}$) of infective AdRGD particles were evaluated by the end-point dilution method using HEK293 cells and expressed as plaque-forming units (PFU).

Gene expression by AdRGD-Luc or conventional Ad-Luc in Meth-A cells. Meth-A cells were plated in 96-well plates at a density of 2×10^3 cells/well and incubated with Ad-Luc or AdRGD-Luc at concentrations of 1250, 2500, 5000, or 10,000 viral particles/cell for 1.5 h. Cells were then washed with PBS and cultured for an additional 48 h. Subsequently, the cells were washed, collected, and lysed with Luciferase Cell Culture Lysis buffer (Promega, USA), and their luciferase activity was measured by the Luciferase Assay System (Promega,

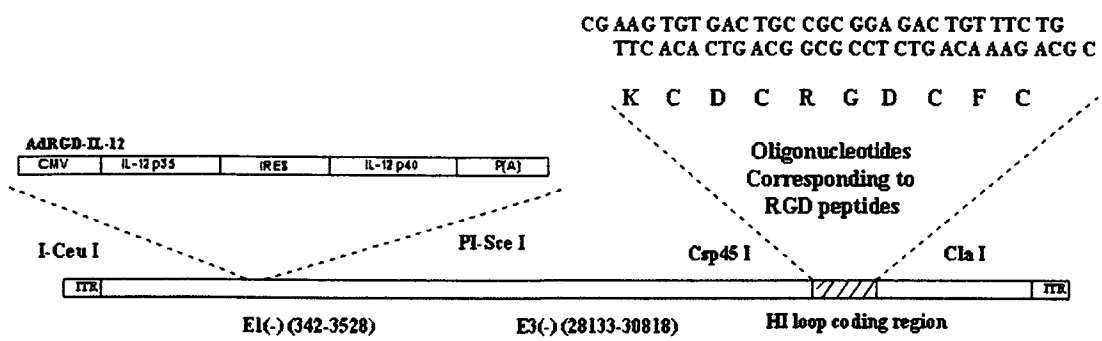

Fig. 1. Construction of IL-12 encoding fiber-mutant adenoviral vector.

USA) and Microlumat Plus LB96 (Perkin-Elmer) according to the manufacturer's instructions.

Analysis of gene transduction of AdRGD-IL-12 in vitro. Meth-A cells were plated in six-well plates at a density of 5×10^5 cells/well and transfected with AdRGD-IL-12 for 24 h at various multiplicities of infection (MOIs) in 2 ml RPMI 1640 medium containing 10% FBS. After three washes of the transfected cells with PBS, a 1.5-ml aliquot of culture medium was added to each well. The supernatants were collected after 24 h, and the amount of IL-12 p70 in each sample was measured with a murine IL-12 p70 ELISA kit (Biosource International, Camarillo, CA, USA) according to the manufacturer's instructions.

Tumor inoculation and intratumoral administration of vectors in animal experiments. Meth-A cells were inoculated intradermally into the flanks of BALB/c mice at 2×10^6 cells/mouse. After 7 days, established tumors (diameter, 9–10 mm) were injected with each vector at 2×10^7 plaque-forming units (PFU) in 50 μl PBS. Tumor size (length and width in mm) was measured twice weekly; animals were euthanized when either of the two parameters exceeded 20 mm. At 3 months after complete regression of the primary tumors, mice were challenged with freshly isolated Meth-A tumor cells or CT26 cells by intradermal injection of 1×10^6 cells into the flank.

Immunohistochemical staining. T-cell infiltration into the Meth-A tumors after intratumoral injection of AdRGD-IL-12 was determined by immunohistochemical analysis. Tumor-bearing mice were euthanized 6 days after administration of AdRGD-IL-12 or the control vector. The tumor nodules were harvested, embedded in OCT compound (Sakura, Torrance, CA, USA), and stored at −80 °C. Frozen thin (6-μm) sections of the nodules were fixed in 4% paraformaldehyde solution, washed with Tris-buffered saline (TBS), and incubated in methanol containing 0.3% hydrogen peroxide for 30 min at room temperature to block endogenous peroxidase activity. The sections were incubated with the optimal dilution of the primary antibody—either rabbit anti-human CD3 antibody (DakoCytomation) or normal rabbit IgG (Santa Cruz Biotechnology)—for 60 min at room temperature. Bound primary antibody was detected after incubation with the secondary antibody from the EnVision+ System (DakoCytomation) for 30 min, followed by a 15-min wash in TBS. The sections were stained with DAB (DakoCytomation) and finally counterstained with hematoxylin (DakoCytomation). We randomly selected six fields from different tumor sections and counted the immunostained cells under a light microscope at 400× magnification.

Experiments on metastatic tumor. We intradermally inoculated mice with 2×10^6 Meth-A cells as described earlier and, 5 days later, injected 8×10^4 cells intravenously. Two days after the intravenous injection, intratumoral injection of AdRGD-IL-12 (2×10^7 PFU) was carried out. The size of the primary tumor was measured twice weekly, and the lungs were harvested 2 weeks after the intravenous injection. The lungs were weighed, sectioned for histology, and stained with hematoxylin and eosin. Metastases in the lungs were identified under a light microscope.

Statistical analysis. Student's t test was used for statistical comparison when applicable. Differences were considered statistically significant at $P < 0.05$.

Results

Meth-A tumor cells transfected with the fiber-mutant adenoviral vector induce higher luciferase gene expression than do those induced with the conventional vector

To evaluate the gene transfection efficiency of the fiber-mutant Ad vector developed for this study, Meth-A cells were transfected with either the conventional Ad-Luc vector or the fiber-mutant AdRGD-Luc vector at various MOIs and the luciferase activity was measured. The luciferase gene expression due to transfection of the fiber-mutant vector was much higher than that from the conventional vector (Fig. 2). For example, at 5000 and 10,000 viral particles/cell, 16.8-fold and 15.7-fold greater gene expression, respectively, was obtained in response to AdRGD-Luc than to Ad-Luc. These results show that insertion of the RGD peptide into the viral fiber enhanced the transfection efficiency of the Ad vector into Meth-A cells.

Expression of IL-12 p70 in Meth-A cells via transfection of AdRGD-IL-12

The IL-12-encoding fiber-mutant adenoviral vector AdRGD-IL-12 was developed as shown in Fig. 1. To confirm the biological activity of AdRGD-IL-12, we used an ELISA to measure the amount of IL-12 in the

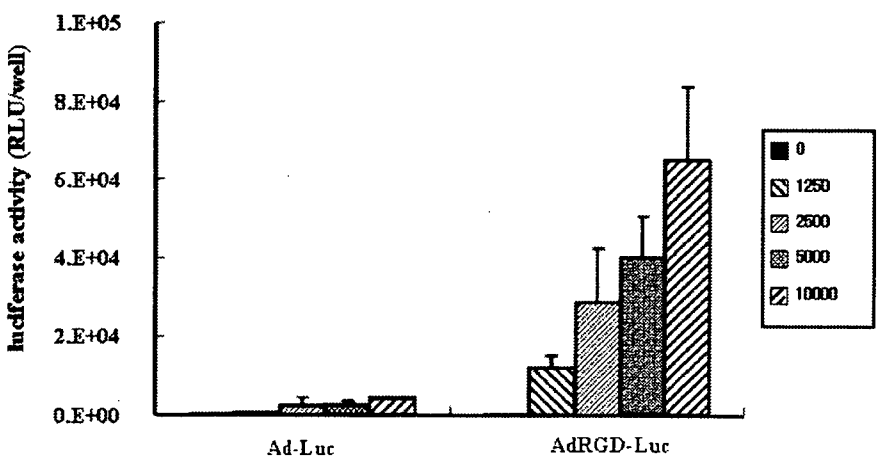

Fig. 2. Gene expression by AdRGD-Luc or conventional Ad-Luc in Meth-A cells. Meth-A cells (2×10^3/well) in 96-well plates were treated with Ad-Luc or AdRGD-Luc at the indicated numbers of viral particles/cell for 1.5 h. Cells were washed and cultured for an additional 48 h. Subsequently, the cells were washed, collected, and their luciferase activity was measured. Data are presented as means ± SE of relative light units (RLUs)/well from three experiments.

supernatants of transfectants. Meth-A cells transfected with AdRGD-IL-12 showed dose-dependent concentrations of IL-12 p70 in the supernatants. In contrast, no detectable IL-12 p70 was present in the culture media of cells that had not been transfected (Fig. 3).

Anti-tumor activity and long-term specific immune response are induced by intratumoral injection of AdRGD-IL-12

The growth of Meth-A tumors was suppressed dramatically, and complete regression occurred in about 70% of the tumor-bearing mice after a single intratumoral injection of 2×10^7 PFU of AdRGD-IL-12. In contrast, the AdRGD-Luc group showed no apparent anti-tumor effect (Fig. 4A). In addition, the relative survival rates further demonstrated prolonged survival after treatment with IL-12 (Fig. 4B). In the rechallenge experiment, mice showing complete regression were reinoculated intradermally with Meth-A or CT26 cells 90 days after the initial injection of tumor cells. All of the mice challenged with Meth-A cells remained tumor-free for at least 2 months (Table 1). In contrast, 100% of the mice challenged with CT26 developed palpable tumors within 2 weeks. These results indicate the generation of specific immunity against Meth-A tumor cells in those mice that rejected Meth-A upon treatment with IL-12.

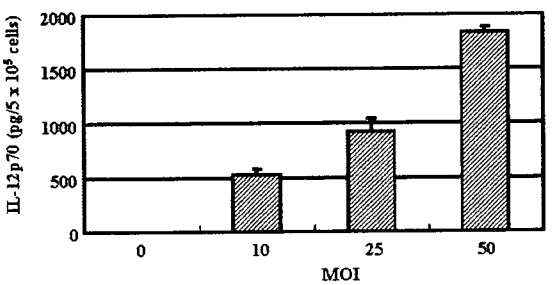

Fig. 3. Production of IL-12 p70 from Meth-A cells transfected with AdRGD-IL-12. We transfected 5×10^5 Meth-A cells with AdRGD-IL-12 for 24 h at the indicated multiplicities of infection (MOIs). Then the cells were cultured for a further 24 h with fresh medium. The supernatants were collected and the IL-12 p70 level was measured by ELISA.

Intratumoral administration of AdRGD-IL-12 induces the infiltration of T cells into Meth-A tumors

To investigate the anti-tumor mechanism of AdRGD-IL-12, tumor tissues were subjected to immunohistochemical staining for CD3 six days after treatment with AdRGD-IL-12 or AdRGD-Luc. Tissues from mice that received AdRGD-IL-12 demonstrated significantly increased accumulation of $CD3^+$ T cells compared
with animals injected with either AdRGD-Luc or PBS (Fig. 5).

Table 1
Specific long-term anti-tumor immune response to IL-12 treatment

Groups	Challenging cell	Tumor rejected mice/challenged mice
Intact mice	Meth-A[a]	0/5
Meth-A rejected[c]	Meth-A[a]	5/5
Meth-A rejected[d]	CT26[b]	0/3

[a] Challenged with 1×10^6 cells.
[b] Challenged with 3×10^5 cells.
[c] Meth-A cured; Meth-A rechallenged.
[d] Meth-A cured; CT26 rechallenged.

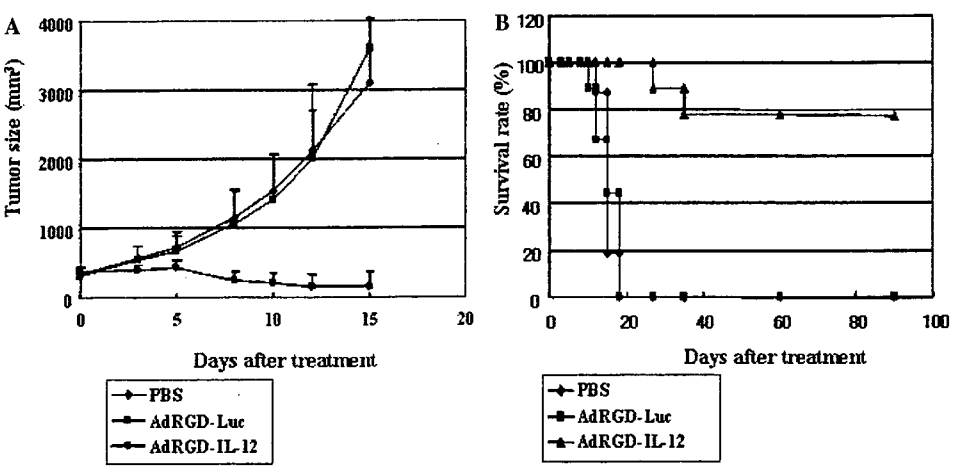

Fig. 4. Growth in BALB/c mice of established Meth-A tumor cells injected intratumorally with IL-12-encoding adenoviral vector. Mice were inoculated intradermally in the flank with 2×10^6 Meth-A cells (100 μl in RPMI 1640). They were then intratumorally injected with 2×10^7 PFU AdRGD-IL-12, AdRGD-Luc, or PBS. Tumor volume was calculated after measuring the length and width of tumors at the indicated time points, and data are expressed as means ± SE of results obtained from at least eight mice. Animals were euthanized when either the length or width of the tumor exceeded 20 mm. (A) Average tumor size. (B) Survival rate (%) of mice.

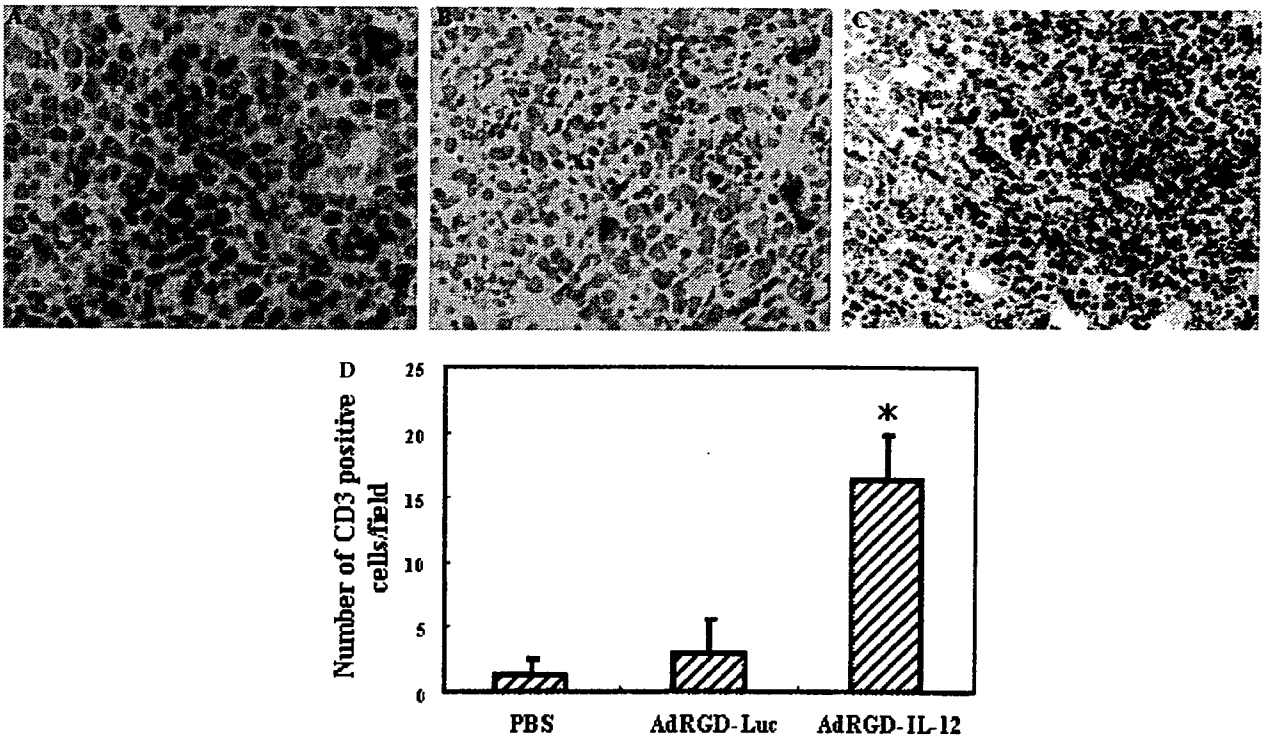

Fig. 5. Intratumoral injection of AdRGD-IL-12 induced the infiltration of $CD3^+$ T cells into Meth-A tumors. Representative views of tumor nodules from mice, harvested 6 days after intratumoral injection of the indicated vectors and controls, and stained for CD3. (A) PBS, (B) AdRGD-Luc, (C) AdRGD-IL-12. The photographs were obtained under light microscopy at 400× magnification. (D) Six fields from different tumor sections were randomly selected and positive cell number infiltrated into tumor tissue was counted. $^*P < 0.05$ with Student's t test in groups between treated with AdRGD-IL-12 and AdRGD-Luc or PBS.

A

Group	Metastasis-free mice/mice in group	Occurrence of Metastasis (%)
PBS	0/8	100%
AdRGD-Luc	1/9	89%
AdRGD-IL-12	8/9	11%

B

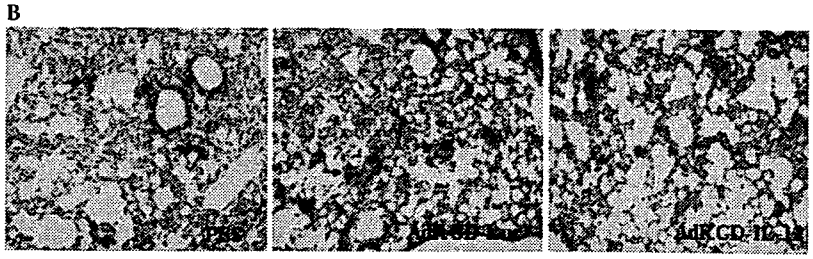

Fig. 6. Anti-metastatic activity due to intratumoral injection of AdRGD-IL-12 into Meth-A fibrosarcoma. (A) Incidence of metastasis in each group. (B) Photomicrographs of lung tissue harvested 2 weeks after treatment and stained with hematoxylin and eosin. The photographs were obtained under light microscopy at 10× magnification. The arrows indicate micrometastasizing tumor.

Anti-metastatic activity is induced by intratumoral injection of AdRGD-IL-12

We then sought to evaluate whether intratumoral injection of AdRGD-IL-12 would induce anti-tumor effects against both the primary and metastatic tumors. Our results showed that single intratumoral injection of AdRGD-IL-12 induced pronounced anti-metastasis activity (Figs. 6A and B) while maintaining tumor-suppressive activity toward the primary tumor, similar to

that shown in Fig. 4 (data not shown). Compared with the control group treated with AdRGD-Luc, in which about 90% of the mice had readily discernable lung metastasis, only one of nine animals treated with AdRGD-IL-12 demonstrated metastasis.

Discussion

Viral vector-encoded chemokines and cytokines are used widely in cancer gene therapy [22,23]. IL-12 has demonstrated remarkable anti-tumor activity when used directly as a recombinant protein or after various viral and non-viral vectors have been used to transfer its genes [24–26]. The development of an efficient vector is pivotal for gene therapy. Because of its high transfection efficiency and because it can transfect both dividing and quiescent cells, Ad vectors are used widely in gene therapy protocols: about 26% of gene therapy clinical trials use Ad vectors as gene carriers [27,28]. However, the lack of Coxsackie adenovirus receptor (CAR), which is an important receptor for conventional Ad vector infection, in many types of malignant cells impairs the tranfection efficiency with Ad vector [29]. Meth-A fibrosarcoma has been confirmed by RT-PCR to be deficient in expression of CAR but with expression of integrin (data not shown). Our previous reports have also shown that insertion of the RGD peptide into the fiber sequences of Ad vectors induces enhanced gene transfection in CT26 and A2058 cells [30,31]. The results of our present study also demonstrate that the fiber-mutant Ad vector induced enhanced expression of the encoded luciferase gene in Meth-A fibrosarcoma cells compared with the expression due to conventional vector (Fig. 2). Furthermore, we confirmed the presence of IL-12 p70 in the supernatant of Meth-A cells transfected with AdRGD-IL-12 (Fig. 3).

Systemic administration of recombinant IL-12 at high doses induces adverse effects associated with high systemic peak concentrations [32,33]. Therefore, gene transfer methods are designed to confine IL-12 production to the tumor environment, thereby preventing systemic toxicity. Tumor cells, dendritic cells, and autologous fibroblasts have been transfected with recombinant adenoviruses or retroviruses to secrete IL-12 locally and have shown favorable efficacy and safety profiles [34,35]. Several groups have shown that intratumoral injection of an Ad vector encoding IL-12 efficiently eradicates experimental gastrointestinal cancer [36,37]. Disadvantages of direct topical administration include tissue damage, and some tumor sites may be inaccessible even to computed tomography-guided percutaneous injection and radiographically directed delivery [38]. However, these limitations favor those types of gene therapy that do not require all tumor cells or tumor masses that express the gene.

Meth-A has shown that it is an IL-12-insensitive tumor cell, in that established tumors could not be treated efficiently via systemic administration of IL-12 and could not even be suppressed effectively (i.e., only 42.5% of mice rejected the tumor) after transfection of an IL-12-containing retroviral vector [12,39]. In our present study, however, a single intratumoral injection of a relatively low dose of AdRGD-IL-12 (2×10^7 PFU) elicited strong anti-tumor activity against established tumors (i.e., diameter of about 10 mm at the beginning of treatment; Fig. 4A). Treatment induced complete tumor regression in about 70% of tumor-bearing mice, and the growth rates of the remaining tumors seem to have been retarded (individual data not shown). Treatment also prolonged the survival of the mice significantly compared with that of the group injected with AdRGD-Luc, a control vector (Fig. 4B). Meanwhile, no detectable IL-12 and IFN-γ existed in the sera after treatment (data not shown)—findings that are consistent with those other reports [40]. Furthermore, intratumoral injection of AdRGD-IL-12 induced a profound long-term specific anti-tumor immunity in mice with complete regression of the initial Meth-A lesion (Table 1).

Studies have shown that IL-12 elicits tumor regression after induction of T-cell migration to tumor sites [41]. The failure of IL-12 therapy in Meth-A via systemic administration is thought to be due to the inability to recruit immune cell migration into tumor cells, and further investigation has indicated a key role of the peritumoral stroma/stromal vasculature in the acceptance of the tumor-infiltrating T cells that are a prerequisite for IL-12-induced tumor regression [12]. Our results similarly demonstrated the accumulation and uniform distribution of $CD3^+$ T cells in the tumor after intratumoral injection, thus supporting the notion that the pronounced anti-tumor effect is related to immune cell infiltration (Fig. 5). However, it remains unclear why intratumoral injection but not systemic administration induces immune cell accumulation in tumor tissue.

We also evaluated the anti-metastasis activity associated with a single intratumoral injection of AdRGD-IL-12. Metastasis is a challenge for cancer treatment, especially because almost all immunotherapy performed in the clinical setting is adjuvant treatment given after surgical reduction of the primary tumor mass for controlling recurrence and metastasis. Interestingly, the single intratumoral injection of AdRGD-IL-12 did induce anti-tumor activity toward disseminated tumors in the lung: histopathology confirmed the complete absence of metastatic tumors in eight of the nine mice tested (and only sporadic residual tumor in the remaining animal). In contrast, all mice that received intratumoral injection of the control vector developed metastases, suggesting that local expression of IL-12 also stimulates the systemic immune response to subsequently affect distant malignant cells.

All the results of our present study indicate that a single intratumoral injection of an IL-12-encoding fiber-mutant Ad vector induces T-cell infiltration into stroma-deficient Meth-A fibrosarcoma and is effective in the treatment of, and protection against challenge with, syngeneic tumors. Our results also suggest that a single intratumoral administration of AdRGD-IL-12 can induce a curative immune response in the face of a micrometastasizing tumor.

Acknowledgments

This study was supported by grants from the Ministry of Health, Labor, and Welfare of Japan and by Grants-in-Aid for Scientific Research on Priority Areas from the Ministry of Education, Culture, Sports, Science and Technology of Japan.

References

[1] M.J. Brunda, Interleukin-12, J. Leukoc. Biol. 55 (1994) 280–288.
[2] G. Trinchieri, Interleukin-12: A proinflammatory cytokine with immunoregulatory functions that bridge innate resistance and antigen-specific adaptive immunity, Annu. Rev. Immunol. 13 (1995) 251–276.
[3] M.P. Colombo, G. Trinchieri, Interleukin-12 in anti-tumor immunity and immunotherapy, Cytokine Growth Factor Rev. 13 (2002) 155–168.
[4] A. Maheshwari, S. Han, R.I. Mahato, S.W. Kim, Biodegradable polymer-based interleukin-12 gene delivery: Role of induced cytokines, tumor infiltrating cells and nitric oxide in anti-tumor activity, Gene Ther. 9 (2002) 1075–1084.
[5] J.W. Yockman, A. Maheshwari, S.O. Han, S.W. Kim, Tumor regression by repeated intratumoral delivery of water soluble lipopolymers/p2CMVmIL-12 complexes, J. Control Release 87 (2003) 177–186.
[6] C.L. Nastala, H.D. Edington, T.G. McKinney, H. Tahara, M.A. Nalesnik, M.J. Brunda, M.K. Gately, S.F. Wolf, R.D. Schreiber, W.J. Storkus, Recombinant IL-12 administration induces tumor regression in association with IFN-γ production, J. Immunol. 153 (1994) 1697–1706.
[7] W.G. Yu, M. Ogawa, J. Mu, K. Umehara, T. Tsujimura, H. Fujiwara, T. Hamaoka, IL-12-induced tumor regression correlates with in situ activity of IFN-gamma produced by tumor-infiltrating cells and its secondary induction of anti-tumor pathways, J. Leukoc. Biol. 62 (1997) 450–457.
[8] J. Cui, T. Shin, T. Kawano, H. Sato, E. Kondo, I. Toura, Y. Kaneko, H. Koseki, M. Kanno, M. Taniguchi, Requirement for valpha 14 NKT cells in IL-12-mediated rejection of tumors, Science 278 (1997) 1623–1626.
[9] M. Iwasaki, W.G. Yu, Y. Uekusa, C. Nakajima, Y.F. Yang, P. Gao, R. Wijesuriya, H. Fujiwara, T. Hamaoka, Differential IL-12 responsiveness of T cells but not of NK cells from tumor-bearing mice in IL-12-responsive versus -unresponsive tumor models, Int. Immunol. 12 (2000) 701–709.
[10] M.J. Smyth, M. Taniguchi, S.E. Street, The anti-tumor activity of IL-12: Mechanisms of innate immunity that are model and dose dependent, J. Immunol. 165 (2000) 2665–2670.
[11] H. Fujiwara, T. Hamaoka, Antitumor and antimetastatic effects of interleukin 12, Cancer Chemother. Pharmacol. 38 (1996) S22–S26.
[12] M. Ogawa, K. Umehara, W.G. Yu, Y. Uekusa, C. Nakajima, T. Tsujimura, T. Kubo, H. Fujiwara, T. Hamaoka, A critical role for a peritumoral stromal reaction in the induction of T-cell migration responsible for interleukin-12-induced tumor regression, Cancer Res. 59 (1999) 1531–1538.
[13] M.J. Brunda, L. Luistro, R.R. Warrier, R.B. Wright, B.R. Hubbard, M. Murphy, S.F. Wolf, M.K. Gately, Antitumor and antimetastasis activity of interleukin 12 against murine tumors, J. Exp. Med. 178 (1993) 1223–1230.
[14] J. Cohen, IL-12 deaths: Explanation and a puzzle, Science 270 (1995) 908.
[15] E.T. Akporiaye, E. Hersh, Clinical aspects of intratumoral gene therapy, Curr. Opin. Mol. Ther. 1 (1999) 443–453.
[16] B. Sangro, G. Mazzolini, J. Ruiz, M. Herraiz, J. Quiroga, I. Herrero, A. Benito, J. Larrache, J. Pueyo, J.C. Subtil, C. Olague, J. Sola, B. Sadaba, C. Lacasa, I. Melero, C. Qian, J. Prieto, Phase 1 trial of intratumoral injection of an adenovirus encoding interleukin-12 for advanced digestive tumors, J. Clin. Oncol. 22 (2004) 1389–1397.
[17] H. Mizuguchi, N. Koizumi, T. Hosono, N. Utoguchi, Y. Watanabe, M.A. Kay, T. Hayakawa, A simplified system for constructing recombinant adenoviral vectors containing heterologous peptides in the HI loop of their fiber knob, Gene Ther. 8 (2001) 730–735.
[18] S. Obana, H. Miyazawa, E. Hara, T. Tamura, H. Nariuchi, M. Takata, S. Fujimoto, H. Yamamoto, Induction of anti-tumor immunity by mouse tumor cells transfected with mouse interleukin-12 gene, Jpn. J. Med. Sci. Biol. 48 (1995) 221–236.
[19] H. Mizuguchi, M.A. Kay, Efficient construction of a recombinant adenovirus vector by an improved in vitro ligation method, Hum. Gene Ther. 9 (1998) 2577–2583.
[20] H. Mizuguchi, M.A. Kay, A simple method for constructing E1- and E1/E4-deleted recombinant adenoviral vectors, Hum. Gene Ther. 10 (1999) 2013–2017.
[21] J.V. Maizel Jr., D.O. White, M.D. Scharff, The polypeptides of adenovirus. I. Evidence for multiple protein components in the virion and a comparison of types 2, 7A, and 12, Virology 36 (1968) 115–125.
[22] J.Q. Gao, Y. Tsuda, K. Katayama, T. Nakayama, Y. Hatanaka, Y. Tani, H. Mizuguchi, T. Hayakawa, O. Yoshie, Y. Tsutsumi, T. Mayumi, S. Nakagawa, Anti-tumor effect by interleukin-11 receptor alpha-locus chemokine/CCL27, introduced into tumor cells through a recombinant adenovirus vector, Cancer Res. 63 (2003) 4420–4425.
[23] R. Dummer, J.C. Hassel, F. Fellenberg, S. Eichmuller, T. Maier, P. Slod, B. Acres, P. Bleuzen, V. Bataille, P. Squiban, G. Burg, M. Urosevic, Adenovirus-mediated intralesional interferon-gamma gene transfer induces tumor regressions in cutaneous lymphomas, Blood 104 (2004) 1631–1638.
[24] A.M. Orengo, E.D. Carlo, A. Comes, M. Fabbi, T. Piazza, M. Cilli, P. Musiani, S. Ferrini, Tumor cells engineered with IL-12 and IL-15 genes induce protective antibody responses in nude mice, J. Immunol. 171 (2003) 569–575.
[25] S. Zheng, G. Zeng, D.S. Wilkes, G.E. Reed, R.C. McGarry, J.N. Eble, L. Cheng, Dendritic cells transfected with interleukin-12 and pulsed with tumor extract inhibit growth of murine prostatic carcinoma in vivo, Prostate 55 (2003) 292–298.
[26] S. Gyorffy, K. Palmer, T.J. Podor, M. Hitt, J. Gauldie, Combined treatment of a murine breast cancer model with type 5 adenovirus vectors expressing murine angiostatin and IL-12: A role for combined anti-angiogenesis and immunotherapy, J. Immunol. 166 (2001) 6212–6217.
[27] Wiley website: <http://www.wiley.co.uk/genmed/clinical>.
[28] J.A. St. George, Gene therapy progress and prospects: Adenoviral vectors, Gene Ther. 10 (2003) 1135–1141.
[29] H. Wu, T. Han, J.T. Lam, C.A. Leath, I. Dmitriev, E. Kashentseva, M.N. Barnes, R.D. Alvarez, D.T. Curiel, Preclinical evalu-

ation of a class of infectivity-enhanced adenoviral vectors in ovarian cancer gene therapy, Gene Ther. 11 (2004) 874–878.

[30] Y. Okada, N. Okada, S. Nakagawa, H. Mizuguchi, K. Takahashi. N. Mizuno, T. Fujita, A. Yamamoto, T. Hayakawa, T. Mayumi, Tumor necrosis factor α-gene therapy for an established murine melanoma using RGD (Arg-Gly-Asp) fiber-mutant adenovirus vectors, Jpn. J. Cancer Res. 93 (2002) 436–444.

[31] J.Q. Gao, S. Inoue, Y. Tsukada, K. Katayama, Y. Eto, S. Kurachi, H. Mizuguchi, T. Hayakawa, Y. Tsutsumi, T. Mayumi, S. Nakagawa, High gene expression of mutant adenovirus vector both in vitro and in vivo with the insertion of integrin-targeting peptide into the fiber, Pharmazie 59 (2004) 571–572.

[32] J.P. Leonard, M.L. Sherman, G.L. Fisher, L.J. Buchanan, G. Larsen, M.B. Atkins, J.A. Sosman, J.P. Dutcher, N.J. Vogelzang, J.L. Ryan, Effects of single-dose interleukin-12 exposure on interleukin-12-associated toxicity and interferon-gamma production, Blood 90 (1997) 2541–2548.

[33] S. Sacco, H. Heremans, B. Hchtenacher, W.A. Buurman, Z. Amraoui, M. Goldman, P. Ghezzi, Protective effect of a single interleukin-12 (IL-12) predose against the toxicity of subsequent chronic IL-12 in mice: Role of cytokines and glucocorticoids, Blood 90 (1997) 4473–4479.

[34] C. Lechanteur, M. Moutschen, F. Princen, M. Lopez, E. Franzen, J. Gielen, V. Bours, M.P. Merville, Antitumoral vaccination with granulocyte-macrophage colony-stimulating factor or interleukin-12-expressing DHD/K12 colon adenocarcinoma cells, Cancer Gene Ther. 7 (2000) 676–682.

[35] L. Zitvogel, B. Couderc, J.I. Mayordomo, P.D. Robbins, M.T. Lotze, W.J. Storkus, IL-12-engineered dendritic cells serve as effective tumor vaccine adjuvants in vivo, Ann. N.Y. Acad. Sci. 795 (1996) 284–293.

[36] G. Mazzolini, C. Qian, X. Xie, Y. Sun, J.J. Lasarte, M. Drozdzik, J. Prieto, Regression of colon cancer and induction of antitumor immunity by intratumoral injection of adenovirus expressing interleukin-12, Cancer Gene Ther. 6 (1999) 514–522.

[37] M. Caruso, K. Pham Nguyen, Y.L. Kwong, B. Xu, K.I. Kosai, M. Finegold, S.L. Woo, S.H. Chen, Adenovirus-mediated interleukin-12 gene therapy for metastasis colon carcinoma, Proc. Natl. Acad. Sci. USA 93 (1996) 11302–11306.

[38] E.T. Akporiaye, E. Hersh, Clinical aspects of intratumoral gene therapy, Curr. Opin. Mol. Ther. 1 (1999) 443–453.

[39] H. Fujiwara, N. Yamauchi, Y. Sato, K. Sasaki, M. Takahashi, T. Okamoto, T. Sato, S. Iyama, Y. Koshita, M. Hirayama, H. Yamagishi, Y. Niitsu, Synergistic suppressive effect of double transfection of tumor necrosis factor-α and interleukin 12 genes on tumorigenicity of Meth-A cells, Jpn. J. Cancer Res. 91 (2000) 1296–1302.

[40] Y. Okada, N. Okada, H. Mizuguchi, K. Takahashi, T. Hayakawa, T. Mayumi, N. Mizuno, Optimization of antitumor efficacy and safety of in vivo cytokine gene therapy using RGD fiber-mutant adenovirus vector for preexisting murine melanoma, Biochim. Biophys. Acta 1670 (2004) 172–180.

[41] G. Mazzolini, J. Prieto, I. Melero, Gene therapy of cancer with interleukin 12, Curr. Pharm. Des. 9 (2003) 1981–1991.

THE JOURNAL OF GENE MEDICINE
J Gene Med 2005; 7: 604–612.
Published online 15 November 2004 in Wiley InterScience (www.interscience.wiley.com). DOI: 10.1002/jgm.699

RESEARCH ARTICLE

PEGylated adenovirus vectors containing RGD peptides on the tip of PEG show high transduction efficiency and antibody evasion ability

Yusuke Eto[1†]
Jian-Qing Gao[1,2†]
Fumiko Sekiguchi[1]
Shinnosuke Kurachi[1]
Kazufumi Katayama[1]
Mitsuko Maeda[4]
Koichi Kawasaki[4]
Hiroyuki Mizuguchi[3]
Takao Hayakawa[3]
Yasuo Tsutsumi[3]
Tadanori Mayumi[4]
Shinsaku Nakagawa[1*]

[1]*Graduate School of Pharmaceutical Sciences, Osaka University, Japan*

[2]*College of Pharmaceutical Sciences, Zhejiang University, P.R. China*

[3]*National Institute of Health Sciences, Japan*

[4]*School of Pharmaceutical Sciences, Kobe Gakuin University, Japan*

*Correspondence to:
Shinsaku Nakagawa, Department of Biopharmaceutics, Graduate School of Pharmaceutical Sciences, Osaka University, Yamadaoka 1-6, Suita City, Osaka 565-0871, Japan.
E-mail:
nakagawa@phs.osaka-u.ac.jp

†These authors contributed equally to this work.

Received: 14 June 2004
Revised: 2 September 2004
Accepted: 2 September 2004

Abstract

Background PEGylation of adenovirus vectors (Ads) is an attractive strategy in gene therapy. Although many types of PEGylated Ad (PEG-Ads), which exhibit antibody evasion activity and long plasma half-life, have been developed, their entry into cells has been prevented by steric hindrance by polyethylene glycol (PEG) chains. Likewise, sufficient gene expression for medical treatment could not be achieved.

Methods A set of PEG-Ads, which have different PEG modification rates, was constructed, and gene expression was evaluated using A549 cells. A novel PEGylated Ad (RGD-PEG-Ad), which contained RGD (Arg-Gly-Asp) peptides on the tip of PEG, was developed. We evaluated gene expression both in Coxsackie-adenovirus receptor (CAR)-positive as well as -negative cells, and *in vivo* gene expression was also determined. Furthermore, the antibody evasion ability and the specificity of infection exhibited by this RGD-PEG-Ad were also evaluated.

Results Whereas PEG-Ads decreased gene expression in CAR-positive cells, RGD-PEG-Ad enhanced gene expression notably, to a level about 200-fold higher than that of PEG-Ads. Moreover, gene expression of RGD-PEG-Ad was almost equal to that of Ad-RGD, which contains an RGD-motif in the fiber and exhibits among the highest gene expression of CAR-positive and -negative cells. Furthermore, although Ad-RGD gene expression decreased remarkably in the presence of anti-Ad antiserum, RGD-PEG-Ad maintained its activity against antibodies. *In vivo* experiments also demonstrated that the modification of Ads with RGD-PEG induced efficient gene expression.

Conclusions In the present study, we demonstrated that a new strategy, which combined integrin-targeting the RGD peptide on the tip of PEG and modified the Ad using this material, could enhance gene expression in both CAR-positive and -negative cells. At the same time, this novel PEGylated Ad maintained strong protective activity against antibodies. This strategy could also be easily modified for developing other vectors using other targeting molecules. Copyright © 2004 John Wiley & Sons, Ltd.

Keywords adenovirus; antibody; polyethylene glycol; RGD peptide; gene expression

Introduction

Gene therapy for cancer or other incurable diseases has attracted considerable attention. The major obstacle to widespread utilization of gene therapy

involves the transgenic vector. Adenovirus vectors (Ads) exhibit high transduction efficiency and gene expression, and can efficiently transfer genes into both dividing and non-dividing cells. Therefore, they are widely used as vectors for gene therapy [1–4]. On the other hand, many people carry neutralizing antibodies to Ads, and the administration of a large amount of Ads may cause side effects. Therefore, clinical application of Ads is difficult [5,6], and many studies have been conducted in an attempt to overcome the limitations of Ads [7–9].

PEGylation, the covalent attachment of activated monomethoxy polyethylene glycol to free lysine groups on the surface of an Ad, is a promising strategy for overcoming these limitations. PEGylation of therapeutic proteins such as cytokines has been reported previously [10,11], and several groups have reported that PEGylated adenovirus exhibits several advantageous attributes [12–14]. Without the need for modifying Ad capsid protein by genetic recombination, a PEGylated Ad (PEG-Ad) can transduce its therapeutic gene into cells even in the presence of Ad-neutralizing antibodies [15,16], and extend residence time in the blood [17]. Furthermore, targeting of PEG-Ads has also been attempted. Lanciotti *et al.* reported targeting Ads using heterofunctional PEG, tresyl-PEG-maleimide [18]. Conjugation of optimized fibroblast growth factor 2 (FGF2), which possesses monoreactive cysteine, to the maleimide group on PEG-Ad was mediated by a reactive sulfhydryl group on the surface of the protein. Ogawara *et al.* reported enhanced transgene delivery to activated vascular endothelial cells using a PEG-Ad combined with an antibody on the tip of PEG [19]. These reports suggest that the use of a functional molecule on the tip of PEG can efficiently change the tropism of Ads or PEG-Ads.

In the present study, we attempted to overcome the previously observed reduction in gene expression caused by the inhibition of endocytosis through the Coxsackie-adenovirus receptor (CAR). This inhibition is due to steric hindrance by the PEG chains and has prevented the widespread therapeutic use of PEG-Ads. Therefore, we developed a new versatile Ad that maintained the positive attributes of PEGylation but also exhibited high transduction efficiency both in CAR-positive and -negative cells.

Infection by Ads occurs in two distinct steps. In the first step, the fiber protein of the Ad binds to its CAR [20–22], and the transduction efficiency of this step is influenced by the amount of CAR present. Following this, internalization via receptor-mediated endocytosis is promoted when the RGD motif of the penton bases combines with $\alpha v\beta 3$ and $\alpha v\beta 5$ integrins [23,24], which are present on many types of cells. We focused on the second step of Ad infection and constructed PEG with RGD peptides on the tip. The PEGylated Ad (RGD-PEG-Ad), which contained RGD peptide on the tip of PEG, was expected to show high transduction efficiency for both CAR-positive and -negative cells because of the interaction between RGD and integrin. Likewise, RGD-PEG-Ad possesses the ability to avoid neutralizing antibodies, a major advantage of PEGylation [15,16]. Incidentally, an Ad that contains an RGD peptide in the HI loop of the fiber (Ad-RGD) has already been developed, and this vector exhibits the highest transduction efficiency via integrin [25,26].

In the present study, we constructed several PEG-Ads at various PEG modification rates, and measured their gene expression. Following this, we used Lipofectamine to determine whether PEG-Ads possessed high gene expression ability. This verified that, upon entering a cell, PEG-Ad expressed the gene originating from the Ad itself. In the next step, we constructed RGD-PEG-Ad and measured its gene expression in CAR-positive and -negative cells with or without Ad antiserum.

Materials and methods

Cell lines

A549 (human lung carcinoma) cells were cultured in Dulbecco's modified Eagle's medium supplemented with 10% fetal calf serum (FCS). B16BL6 (mouse melanoma) cells were cultured in minimum essential medium supplemented with 7.5% FCS.

Development of adenovirus vectors

In this study, all experiments used E1-deleted Ad type 5, which expressed firefly luciferase under the control of cytomegalovirus (CMV) promoters. Both conventional and RGD fiber mutant Ads were amplified in 293 cells using a modification of established methods, purified from cell lysates by banding twice through CsCl gradients, dialyzed and stored at −80 °C. The Ads used in this study were constructed by an improved *in vitro* ligation method as described previously [27]. Determination of virus particle titer was accomplished spectrophotometrically by the methods of Maizel *et al.* [28].

Preparation of RGD-PEG

The synthetic scheme for RGD-PEG is shown in Figure 3. *N*-(9-Fluorenylmethoxycarbonyl)-*O*-(succimidyl)-ω-amino-α-carboxy-PEG (Fmoc-PEG-NHS, MW 3400) was purchased from Shearwater Corporation (USA). β-Ala (βA) was used as a spacer between PEG and the RGD peptide. (Ac-YGGRGDTPβA)$_2$K-PEG-βAC-amide (RGD-PEG, MW 5500) was synthesized manually on a Rink amide resin [29] using a 9-fluorenylmethoxycarbonyl (Fmoc)-based solid-phase strategy. We employed 2(1*H*-benzotriazol-1-yl)-1,1,3,3-tetramethyluronium hexafluorophosphate and 1-hydroxybenzotriazole as coupling reagents, trityl (Trt) protection as the sulfhydryl group source, *tert*-butyl as the hydroxyl group source and 2,2,5,7,8-pentamethylchroman-6-sulfonyl (Pmc) protection as the guanidinyl group source. To liberate the synthetic RGD-PEG from the resin, cleavage was achieved by using

a mixture of trifluoroacetic acid/triisopropylsilane/H_2O (95 : 2.5 : 2.5) [30] for 2 h at room temperature, followed by high-performance liquid chromatography (HPLC) purification on a C18 column. After addition of the peptide to *N*-(6-maleimidecaproyloxy)succinimide) (EMCS) in phosphate-buffered saline (PBS), pH 6.4, the solution was changed to pH 7.4 PBS and kept frozen at −80 °C.

Covalent attachment of PEG to Ads

Activated methoxypolyethylene glycol-succinimidyl propionate (mPEG-SPA, MW 5000; Shearwater Corporation, USA) and RGD-PEG were used in this study. Ads were reacted with 25–6400-fold molar excess of mPEG-SPA to viral lysine residue at 37 °C for 45 min with gentle stirring. Ads were also reacted with 250-fold molar excess of RGD-PEG under the same conditions. CsCl gradient ultracentrifugation was used for PEGylated adenovirus purification, and we assessed whether unmodified Ads were mixed with the PEGylated Ad. Modification ratio of PEGylated-Ads was determined by sodium dodecyl sulfate/polyacrylamide gel electrophoresis (SDS-PAGE) analysis using NIH image software. SDS-PAGE was carried out, referring to the previous report by O'Riordan *et al.* [15], in a 4–20% polyacrylamide gel (PAG Mini 4/20; Daiichi Pure Chemicals, Japan). Viral protein (hexon) was stained by Coomassie brilliant blue. The PEGylated hexon band was separated from the unmodified hexon band. The ratios of each band were measured using NIH Image software, and the PEG modification ratio was calculated as described below, the band of PEGylated hexon/the band of PEGylated and unmodified hexon ×100 [16]. After dilution in PBS, the particle sizes of Ads and RGD-PEG-Ad were measured using a Zetasizer 3000HS (Malvern Inc. UK).

Transduction efficiency of PEGylated Ads into A549 cells

A549 cells (2×10^4 cells/well) were seeded onto a 48-well plate. On the following day, the cells were transduced with 300, 1000, 3000, or 10 000 particles/cell of unmodified Ads and PEG-Ads that possessed various PEG modifications in a final volume of 500 µl in cell medium. After 24 h cultivation, luciferase activity was measured using the luciferase assay system (Promega, USA) and Microlumat Plus LB 96 (Perkin Elmer, USA) after cells had been lysed with the luciferase cell culture lysis reagent (Promega, USA). Luciferase activity was calculated as relative light units (RLU)/well. In the presence of 20 µg/ml Lipofectamine 2000 (Invitrogen, USA), A549 cells were transduced with 1000 particles/cell of unmodified Ads, 43%, 72%, and 89% modified PEG-Ads, heatinactivated Ads, or heat-inactivated PEG-Ads, respectively. After 4 h, the virus solution was replaced with fresh medium, and the cells were incubated for 24 h. Subsequently, luciferase expression was measured using the method described above.

Transduction efficiency of RGD-PEG-Ad into A549 and B16BL6 cells

A549 and B16BL6 cells (2×10^4 cells/well) were seeded onto a 48-well plate. On the following day, the cells were transduced with 300, 1000, 3000, and 10 000 particles/cell of unmodified Ads, PEG-Ads, RGD-PEG-Ad or Ad-RGD, respectively, in a final volume of 500 µl in cell medium. After 24 h cultivation, luciferase activity was measured using the method described above.

Competition experiments using RGD peptide

B16BL6 cells (2×10^4 cells/well) were seeded onto a 48-well plate. On the following day, cells were incubated with RGD peptide (GRGDTP, SIGMA) at a final concentration of 200 µg/ml for 10 min at room temperature, and then 3000 particles/cell of unmodified Ads, RGD-PEG-Ad or Ad-RGD were added to a final volume of 300 µl in cell medium. After 24 h cultivation, luciferase activity was measured using the method described above.

Preparation of Ad antiserum

Ad antiserum was obtained from ICR mice using methods previously reported by us and others [16,31]. In brief, a dose of 10^{10} particles of unmodified Ad containing Freund's complete adjuvant in 100 µl of PBS was administered hypodermically to a female ICR mouse (6 weeks old). Two to four weeks later, an additional dose of 10^{10} viral particles in Freund's incomplete adjuvant was hypodermically administered. Mouse serum was collected after 1 week, and stored at −20 °C.

Antibody evasion by RGD-PEG-Ad in B16BL6 cells

B16BL6 cells (2×10^4 cells/well) were seeded onto a 48-well plate. On the following day, the cells were transduced with 1000 particles/cell of RGD-PEG-Ad or Ad-RGD in a final volume of 500 µl in cell medium in the presence or absence of 100 µl/well Ad antiserum (42, 125 ng protein/well). After 24 h cultivation, luciferase activity was measured using the method described above.

Ad-mediated gene transduction *in vivo*

Unmodified Ad, Ad-RGD, and RGD-PEG-Ad (1.5×10^{10} particles/100 µl) were intravenously injected into BALB/c mice (female, 6 weeks old; obtained from Nippon SLC, Kyoto, Japan). Forty-eight hours later, organs were isolated and homogenized as previously described [32]. Luciferase activity was measured using the method described above.

Statistical analysis

Student's t-test was used for statistical comparison when applicable. Differences were considered statistically significant at $P \leq 0.05$.

Results

Transduction efficiency of Ads declines in response to PEGylation

We confirmed the feasibility of constructing PEG-Ads that exhibit various PEG modification rates, which are regulated by the amount of PEG made available for the reaction (data not shown). In the present study, Ads were reacted with 25-, 100-, 400-, 1600- and 6400-fold molar excesses of PEG relative to viral lysine residue. The results showed that the transduction efficiency of PEG-Ads fell remarkably as the PEG modification rate increased (Figure 1). Luciferase expression of the 34% modified PEG-Ad was approximately 200-fold lower than that of unmodified Ads, and gene expression of the 89% modified PEG-Ad fell by 100 000 or more and was not dose-dependent.

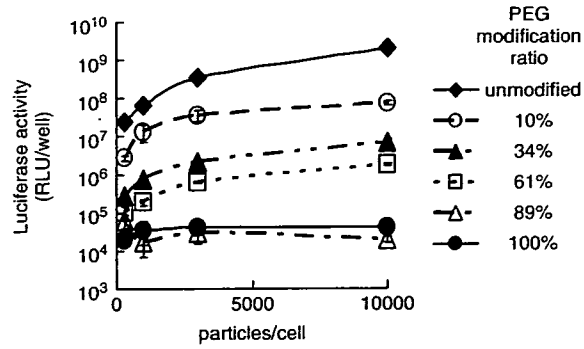

Figure 1. Transduction efficiency of PEGylated adenovirus vectors into A549 cells. A549 cells (2×10^4 cells) were transduced with 300, 1000, 3000 or 10 000 particles/cell of unmodified Ad or PEG-Ad encoding the luciferase gene at the indicated modification ratios. Luciferase expression was measured after 24 h. Each point represents the mean ± S.D. (n = 3)

PEG-Ads show high gene expression upon cell entry

We introduced PEG-Ads into cells using Lipofectamine and measured their gene expression in order to verify that the decrease of gene expression of PEG-Ads was derived from binding inhibition due to steric hindrance by PEG chains. The results shown in Figure 2 demonstrated that, in the absence of Lipofectamine, the transduction efficiency of PEG-Ads significantly decreased as PEG modification rate increased. However, in the presence of Lipofectamine, PEG-Ad gene expression at 43% modification was enhanced significantly to nearly that of unmodified Ads. Even at high modification rates (89%), the PEG-Ad gene expression in the presence of Lipofectamine was more than 130-fold higher than that in the absence of Lipofectamine. The gene expression of the heat-inactivated unmodified Ads and the heat-inactivated PEG-Ads were very low even with Lipofectamine. The results

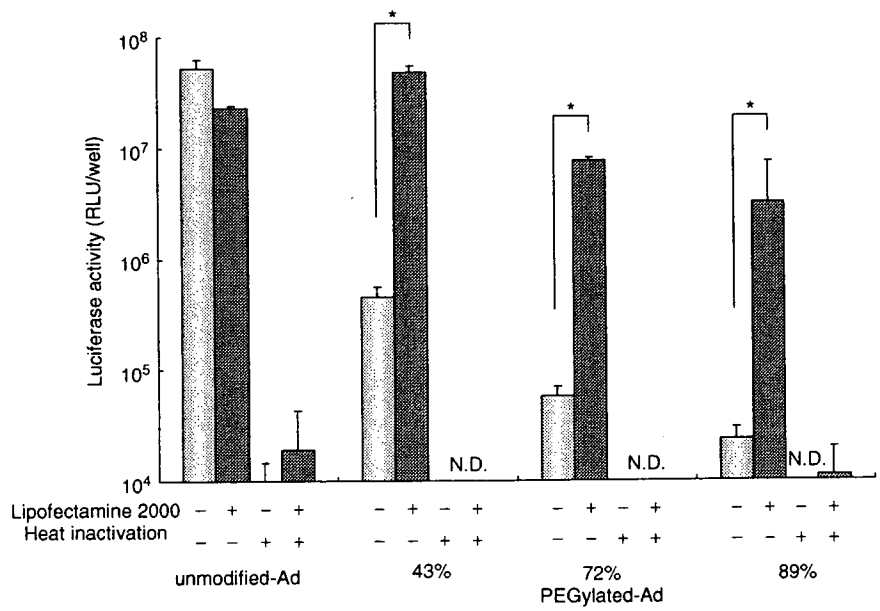

Figure 2. Transduction efficiency of PEGylated adenovirus vectors into A549 cells in the presence or absence of Lipofectamine 2000. A549 cells (2×10^4 cells) were transduced with 1000 particles/cell of unmodified Ad or PEG-Ad in the presence or absence of 20 μg/ml of Lipofectamine 2000. After 4 h, the virus solution was replaced with fresh medium, and the cells were incubated for 24 h. Luciferase expression was measured. Each point represents the mean ± S.D. (n = 3). *$P < 0.05$ (Student's t-test)

shown here indicate that high transduction efficiency, which is characteristic of Ads, decreased due to the steric hindrance of CAR by PEG chains.

Construction of PEGylated Ads with RGD peptides

In selecting the adhesion molecule, we focused on the RGD motif, the second mediator of Ad internalization. We constructed RGD-PEG-Ad using RGD-PEG-NHS (Figure 3), which contains two RGD motifs (YGGRGDTP) on the tip of PEG, and we investigated the characteristics of RGD-PEG-Ad (Table 1). RGD-PEG-Ad was 12.5 nm bigger in diameter than unmodified Ads, and the PEG modification rate (36%) was confirmed by SDS-PAGE and NIH Image software.

Enhanced transduction efficiency of RGD-PEG-Ad in comparison to that induced by PEG-Ads

We compared the transduction efficiency of unmodified Ads, PEG-Ads, Ad-RGD, and RGD-PEG-Ad in both A549 (CAR-positive) and B16BL6 (CAR-negative) cells. In A549 cells, RGD-PEG-Ad showed 100-fold higher gene expression than PEG-Ad, which exhibits the same level of modification. This gene expression level was similar to that of unmodified Ads and Ad-RGD (Figure 4A). In B16BL6 cells, RGD-PEG-Ad exhibited 60-fold and 200-fold higher gene expression rates than unmodified Ad and PEG-Ad, respectively, but the expression rate was similar to that of Ad-RGD (Figure 4B).

Table 1. Modification ratio and vectors size of RGD-PEG-Ad

Ratio (Ad/RGD-PEG)*	PEG modification ratio (%)	Vector size (nm)
1:0 (unmodified)	0	122.1 ± 4.5
1:250	36	134.6 ± 2.7

*Amount of PEG to lysine residue of adenovirus vector capsid protein (mol/mol)

RGD-PEG-Ad specifically infect cells through integrin

The specificity of RGD-PEG-Ad binding via integrin was evaluated by competition assay using the RGD peptide, GRGDTP, which has been widely used as a competitive peptide for integrin [33,34]. In the presence of GRGDTP, RGD-PEG-Ad and Ad-RGD gene expression was remarkably decreased compared to that in the absence of RGD peptide (Figure 5). In contrast, unmodified Ad did not decrease notably, suggesting the introduction of RGD-PEG-Ad was integrin-dependent.

RGD-PEG-Ad maintains its high gene expression in the presence of Ad antiserum

We evaluated transduction efficiency of Ad-RGD and RGD-PEG-Ad in the presence or absence of Ad antiserum using B16BL6 cells. In the presence of Ad antiserum, Ad-RGD gene expression was reduced remarkably. However, RGD-PEG-Ad maintained its high transduction efficiency (Figure 6). In the presence of 125 ng anti-Ad antibody,

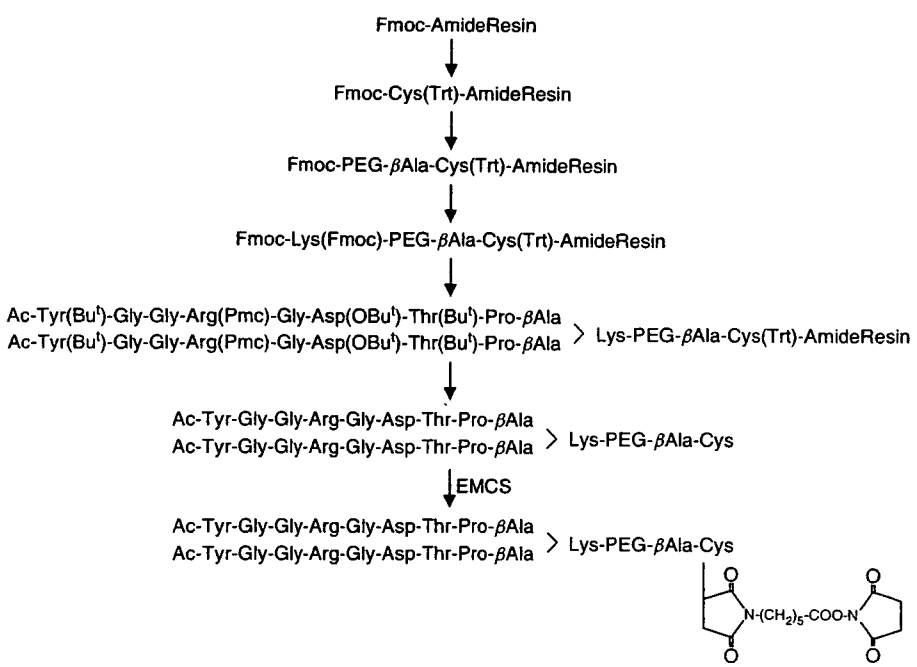

Figure 3. Structural scheme for RGD-PEG